F. Tatsuoka, M. Tateyama, T. Uchimura and J. Koseki

GEOSYNTHETIC-REINFORCED SOIL RETAINING WALLS AS IMPORTANT PERMANENT STRUCTURES

1996-1997 MERCER LECTURE

ABSTRACT: During the past decade, more than 26 km of geosynthetic-reinforced soil retaining walls (GRS-RWs) with full-height rigid (FHR) facings were constructed in Japan as important permanent structures mainly for railways and occasionally for highways. These include retaining walls for embankments, bridge abutments, a wall backfilled with a nearly saturated clay constructed on a thick soft clay deposit, a wall that survived a very severe earthquake, and walls constructed to support bullet train tracks. The full-height rigid facings are cast in place using staged construction procedures. A new method of stiffening reinforced soil by vertical preloading and prestressing is also described.

KEYWORDS: Geosynthetic, Reinforced soil retaining wall, Full-height rigid facing, Staged construction, Case histories, Railway, Highway, Bridge abutment and pier, Permanent structure.

AUTHORS: F. Tatsuoka, Professor, Department of Civil Engineering, University of Tokyo, 7-3-1, Hongo, Bunkyo-ku, Tokyo, 113, Japan, Telephone: 81/3-3812-2111, Ext. 6120, Telefax: 81/3-5689-7268, E-mail: tatsuok@hongo.ecc.u-tokyo.ac.jp; M. Tateyama, Senior Research Engineer, Railway Technical Research Institute, 2-8-38, Hikarimachi, Kokubunji, Tokyo, 185, Japan, Telephone: 81/425-73-7261, Telefax: 81/425-73-7248, E-mail: tate@rtri.or.jp; T. Uchimura, Research Assistant, Department of Civil Engineering, University of Tokyo, 7-3-1, Hongo, Bunkyo-ku, Tokyo, 113, Japan, Telephone: 81/3-3812-2111, Ext. 6122, Telefax: 81/3-5689-7268, E-mail: uchimura@civil.t.u-tokyo.ac.jp; and J. Koseki, Associate Professor, Institute of Industrial Science, University of Tokyo, 7-22-1, Roppongi, Minato-ku, Tokyo, 106, Japan, Telephone: 81/3-3402-6231, Telefax: 81/3-3479-0261, E-mail: koseki@iis.u-tokyo.ac.jp.

PUBLICATION: *Geosynthetics International* is published by the Industrial Fabrics Association International, 345 Cedar St., Suite 800, St. Paul, Minnesota 55101-1088, USA, Telephone: 1/612-222-2508, Telefax: 1/612-222-8215. *Geosynthetics International* is registered under ISSN 1072-6349.

DATES: Original manuscript received 8 March 1997 and accepted 11 April 1997. Discussion open until 1 January 1998.

REFERENCE: Tatsuoka, F., Tateyama, M., Uchimura, T. and Koseki, J., 1997, "Geosynthetic-Reinforced Soil Retaining Walls as Important Permanent Structures", *Geosynthetics International*, Vol. 4, No. 2, pp. 81-136.

1 INTRODUCTION

1.1 Geosynthetic-Reinforced Soil Retaining Walls (GRS-RWs) With Full-Height Rigid (FHR) Facings

A construction system for "permanent" geosynthetic-reinforced soil retaining walls (GRS-RWs) is now widely used in Japan. This system is characterized by the following features:

- The use of a full-height rigid (FHR) facing that is cast in place using staged construction procedures (Figure 1).
- The use of polymer geogrid reinforcement for cohesionless soils to provide good interlock with the soil, and the use of a composite of nonwoven and woven geotextiles for nearly saturated cohesive soils to facilitate both drainage and tensile reinforcement of the backfill.
- The use of relatively short reinforcement.
- The use of low-quality on-site soil as the backfill, if necessary.

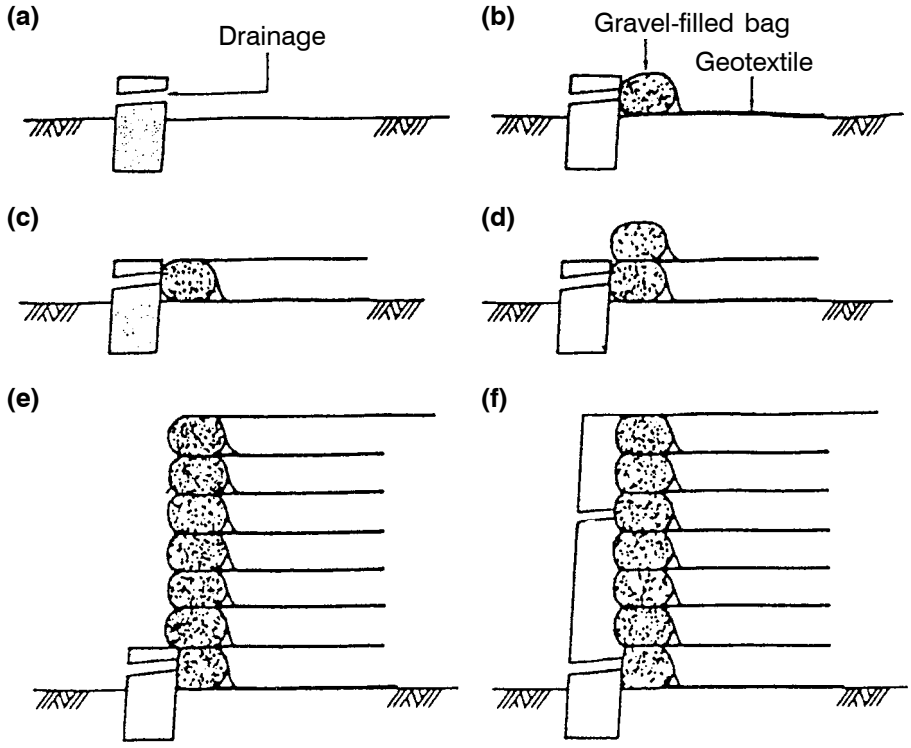

Figure 1. Standard staged construction procedure for a GRS-RW: (a) concrete base; (b) geotextile and gravel-filled bag placement; (c) backfill and compaction; (d) placement of the second layer of geotextile and a gravel-filled bag; (e) all layers constructed; (f) concrete facing constructed.

The staged construction method (Figure 1) consists of the following steps:

1. a small foundation for the facing is constructed;
2. a geosynthetic-reinforced soil wall with a wrap-around wall face is constructed using gravel-filled bags placed at the shoulder of each soil layer; and
3. a thin and lightly steel-reinforced concrete facing is cast in place directly adjacent to the wall face after deformation of the backfill and the subsoil layer beneath the wall has occurred, and a good connection is made between the facing and the main body of the wall.

1.2 A Typical Recent Case History

Figure 2 shows a recent GRS-RW project with a FHR facing in Japan. The wall supports the main tracks of a new bullet train line (Hokuriku Shinkansen), which is now under construction between the north of Tokyo and Nagano City, Japan, where the winter Olympic games will be held in 1998. The wall is 4.6 to 8.6 m high and 260 m long extending between a bridge abutment and a tunnel exit. The completed wall looks like a conventional reinforced concrete (RC) cantilever wall (Figure 2c). The backfill is a well-graded crushed gravel reinforced with a polyester geogrid coated with polyvinyl chloride (PVC). The reinforcement comes in two types having a rupture strength T_R = 35.3 kN/m and 68.6 kN/m for relatively low and high walls, respectively. This is one of the first walls to directly support the main tracks of a bullet train. Retaining walls supporting bullet train foundations are some of the most critical civil engineering structures in Japan. For this new line, GRS-RWs with FHR facings were constructed at 11 sites comprising a total length of 3,330 m. This includes the walls constructed at a railway yard in Nagano City, which are described in Section 3.

1.3 Brief History

The study of the GRS-RW system started in 1982. Since 1987, and particularly since its approval in 1992 by the Ministry of Transport of Japan, a large number of permanent GRS-RWs with FHR facings (typically 5 m high) have been constructed to support more than 26 km of important railway tracks as of April 1997 (Figure 3). Two typical large-scale railway application projects are in Nagoya (Location 4, Figure 3; Tateyama et al. 1994b) and Amagasaki (Location 7, Figure 3; Kanazawa et al. 1994). More than 760 m of GRS-RWs with FHR facings have been constructed to support highways. The most recent large GRS-RW with a FHR facing project is in Yamagata Minami (Location 60, Figure 3) where the Japan Highway Authority is reconstructing an embankment slope to widen a highway lane (Tada et al. 1997). The greatest wall height is 11.3 m and the total wall length is 240 m. The stability of GRS-RW systems has been validated by the excellent post-construction performance of these walls (Tatsuoka et al. 1992, 1996a; Murata et al. 1991, 1994; Kanazawa et al. 1994; Doi et al. 1994).

Before the GRS-RW construction system was introduced, the Terre Armée technique dominated the permanent reinforced-soil retaining wall market in Japan. Japan National Railways, the predecessor organization to Japan Railways (JR), was the first nationwide organization that extensively constructed Terre Armée walls. However, many conventional GRS-RWs with wrap-around wall faces had been constructed, but only

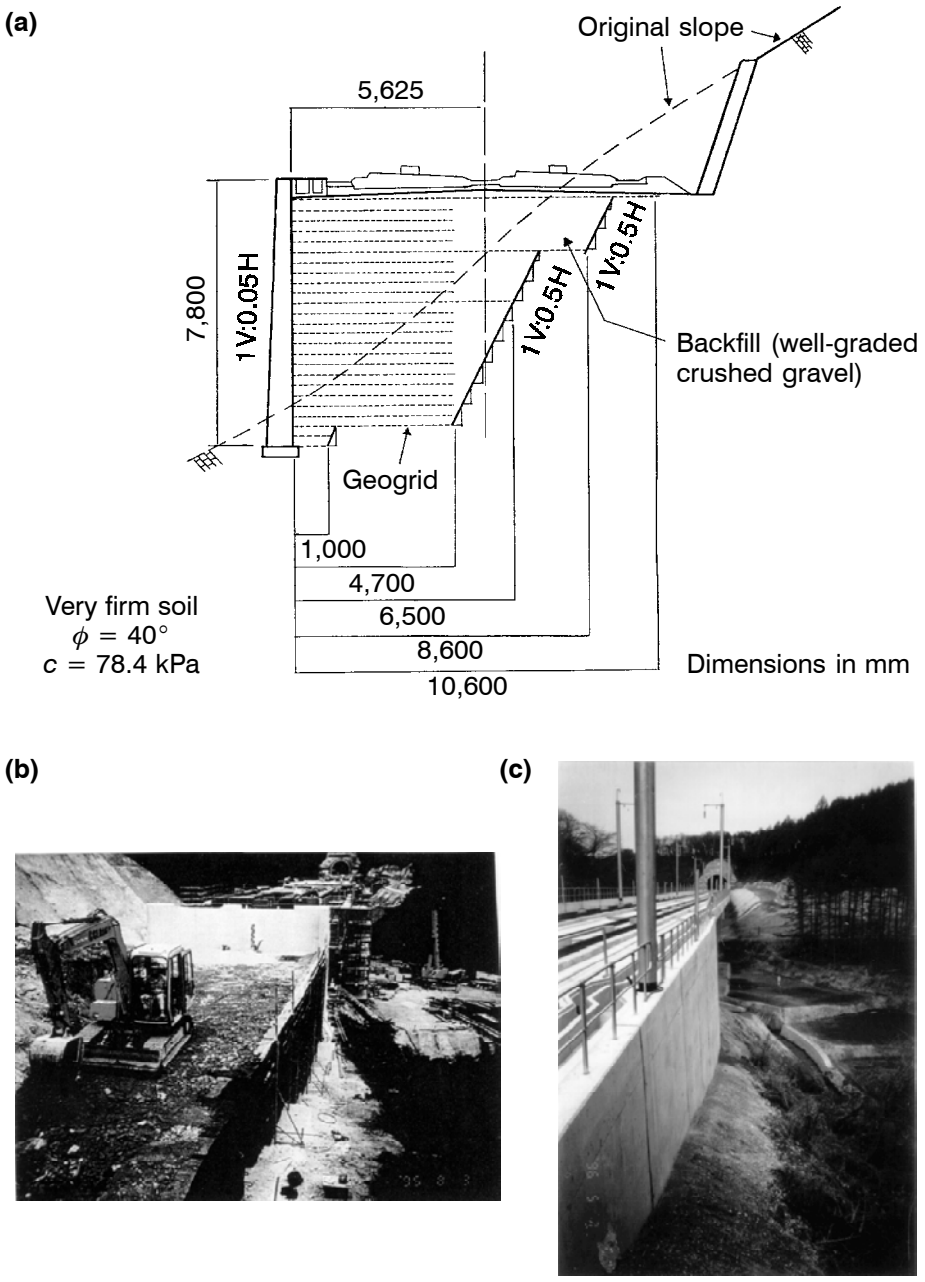

Figure 2. GRS-RW with a FHR facing constructed to support bullet train tracks (Hokuriku Shinkansen) west of Karuizawa (Location 50, Figure 3): (a) typical cross section (gravel-filled gabions are not shown); (b) wall under construction; (c) completed wall.

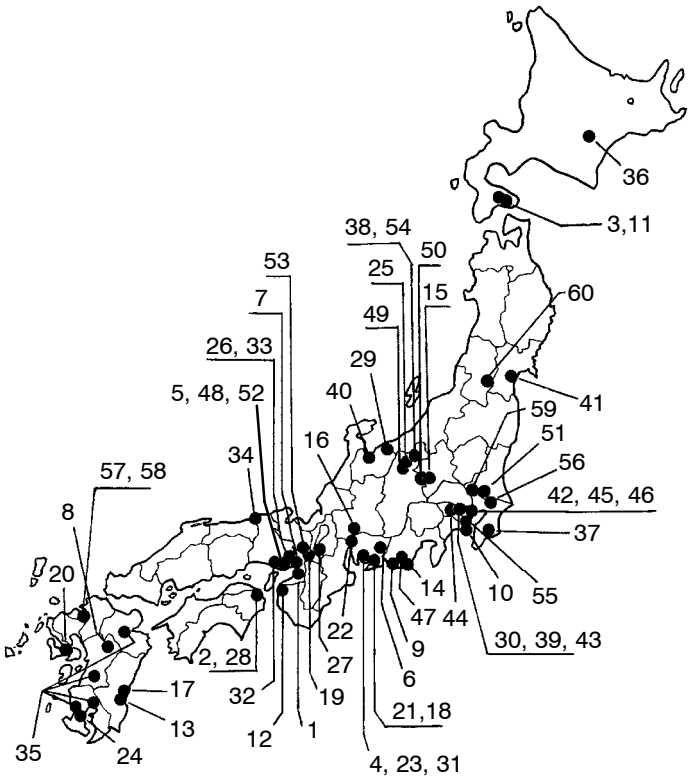

Figure 3. Locations of the major GRS-RW projects in Japan (numbered in chronological order).

as temporary walls or for secondary applications, and not for permanent railway related structures. Today, in Japan, the use of the Terre Armée construction technique for railway support structures has declined, and the use of GRS-RWs with FHR facings has become more common (Tatsuoka et al. 1994). In the current JR design standard for soil retaining structures, the GRS-RW and Terre Armée wall systems, in addition to other conventional techniques, are specified design and construction methods, thus providing the designer with a choice. In many railway projects, however, the GRS-RW system has been adopted instead of conventional RC retaining wall techniques and the Terre Armée technique.

Among the project locations shown in Figure 3, the following recent projects will be discussed in this paper: "Seibu Bridge Abutments" (Location 42); "Nagano Wall", which uses a nearly saturated backfill soil constructed on a very soft clay deposit (Location 38); "railway embankments" damaged by flood and reconstructed using the GRS-RW system in southern Kyushu (Location 35); and "Tanata Wall" (Location 5) which survived a severe earthquake. The important lessons learned from these case histories involve the following issues:

1. cost performance;

2. wall deformability;
3. wall stability; and,
4. durability and acceptable aesthetics of the wall face.

Issues 1 to 4 are discussed by comparing GRS-RWs with FHR facings to conventional retaining walls and conventional steel-reinforced soil retaining walls. The issue of geosynthetic reinforcement durability is beyond the scope of this paper.

2 LOW COST/PERFORMANCE RATIO

2.1 Can the Facing be Simpler?

It is known that reinforced soil retaining wall systems in general are cost-effective because the facing structure is much simpler than that of most conventional retaining wall systems, which results in lower construction cost, higher construction speed and use of lighter construction machines. In addition, the wall performance is equivalent to, or better than conventional retaining wall systems. In addition, for flexible walls, the pile foundation that supports the facing of conventional retaining wall systems becomes unnecessary, resulting in a more cost-effective system.

Using the design earth pressure, which is usually the active earth pressure, P_A , in the unreinforced backfill, a conventional retaining wall is designed as a cantilever structure supported at its base (Figure 4a). Large internal moment and shear forces may be mobilized in the facing structure, and a large overturning moment and sliding force may develop at the bottom of the wall structure. In the case of a reinforced soil retaining wall, the backfill is retained by the tensile force in the reinforcement (Figure 4b). The conventional explanation, which is misleading, says that because of this reinforcement effect only very small earth pressures act on the back of the facing, and accordingly only a light and flexible facing is required to contain the backfill soil.

Realistically, however, the earth pressure acting on the back of the facing can never approach zero unless the backfill soil is very cohesive, or unless a large amount of soil arching develops between two vertically adjacent reinforcement layers. Soil arching is most likely to develop at the lower reinforcement layers in a wall. If the earth pressure activated on the back of the facing is approximately zero, there must be zero tensile force at the connection between the reinforcement and the back of the facing, which results in a large reduction of the soil retaining capability of the reinforcement (Figure 5a) (Tatsuoka 1993). Consequently, as the lateral confining pressure on the soil in the active zone decreases, the active zone becomes more deformable and less stable, particularly when the backfill is a cohesionless soil.

The above concept can be explained using the following expression to calculate the maximum available tensile force, T_{max} , in each reinforcement member:

$$T_{max} = \text{Minimum of } [T_R,\ T_{anchor},\ T_{retain} + T_{W\,max}] \tag{1}$$

where: T_R = tensile rupture strength of each reinforcement layer; T_{anchor} = anchorage capacity, which is approximately proportional to the anchorage length, L_a ; T_{retain} = avail-

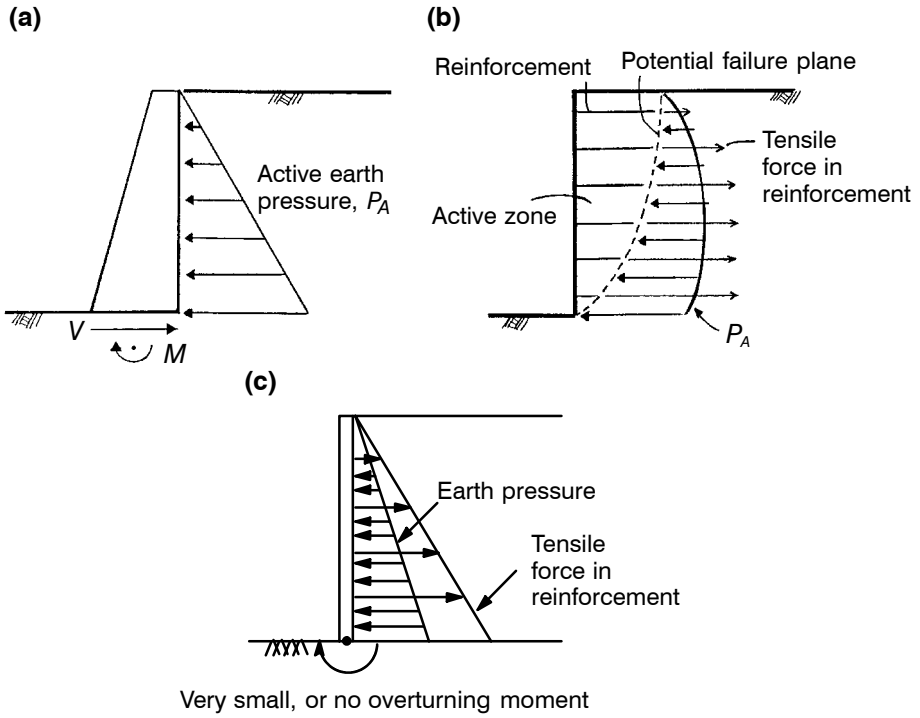

Figure 4. Force equilibrium for: (a) a conventional retaining wall; (b) a reinforced soil retaining wall; (c) the FHR facing of a GRS-RW.

able retaining strength, which is approximately proportional to the retaining length, L_r; and, T_{Wmax} = available tensile force at the connection between the reinforcement and the back of the facing, which increases with an increase in the available earth pressure on the back of the facing. As the connection strength, T_{Wmax}, decreases to zero, the distribution of the reinforcement tensile force, T, is represented by B1 and B2 in Figure 5b. Thus, at lower levels in the wall, the maximum available tensile force in each reinforcement member, T_{max}, is not large enough, while a large T_{Wmax} value results in a large T_{max} value (i.e. the reinforcement tensile force distribution A2 in Figure 5b). In Figure 5b, it is assumed that for distributions A1 and A2, the active zone is confined without exhibiting large strains, and therefore, large bond stresses are not mobilized at the surface of the reinforcement in the active zone. In this case, the reinforcement tensile force, T, is constant in the active zone. For the distributions B1 and B2, a small value of $T_{(max)B2}$ may result in either a value of $T_{(max)B1}$ larger than $T_{(max)A1}$ for a fixed potential failure plane (in the case of Figure 5b) (Jewell 1990) or a longer retaining length, L_r, with a larger deformable active zone to increase $T_{(max)B2}$ to a value similar to $T_{(max)A2}$, mobilized at reinforcement locations further from the wall face.

The results of a number of field and laboratory tests, numerical analyses, and the behavior of many full-scale walls have shown that the earth pressure on the back of the

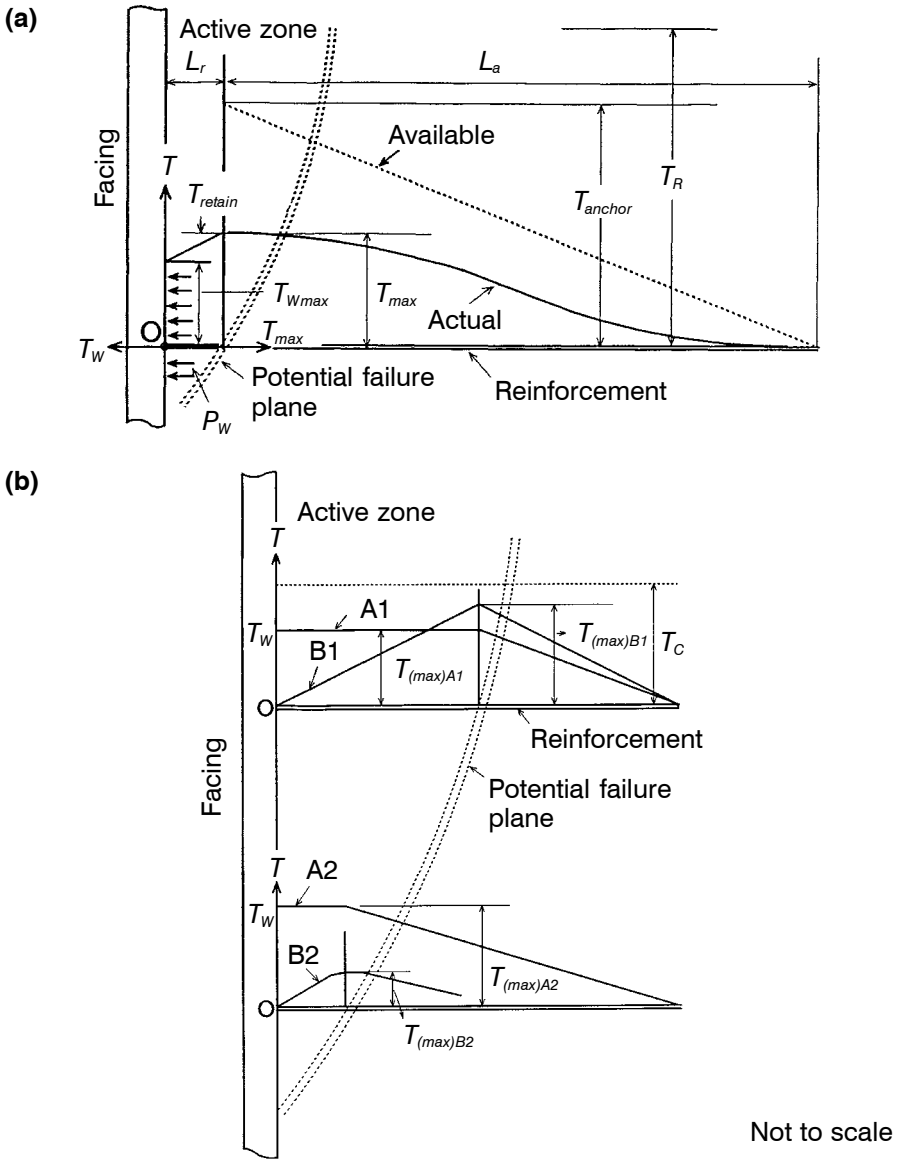

Figure 5. Tensile force distribution in the reinforcement layers for a reinforced soil retaining wall: (a) available maximum tensile force in the reinforcement; (b) two extreme tensile force distributions in the reinforcement (Tatsuoka 1993).

facing increases with an increase in facing rigidity (e.g. Figures 4.1 and 4.2 of Tatsuoka 1993). Figure 6 shows the results of a relatively large-scale plane strain laboratory model GRS-RW test performed under well-controlled conditions (Tajiri et al. 1996). The

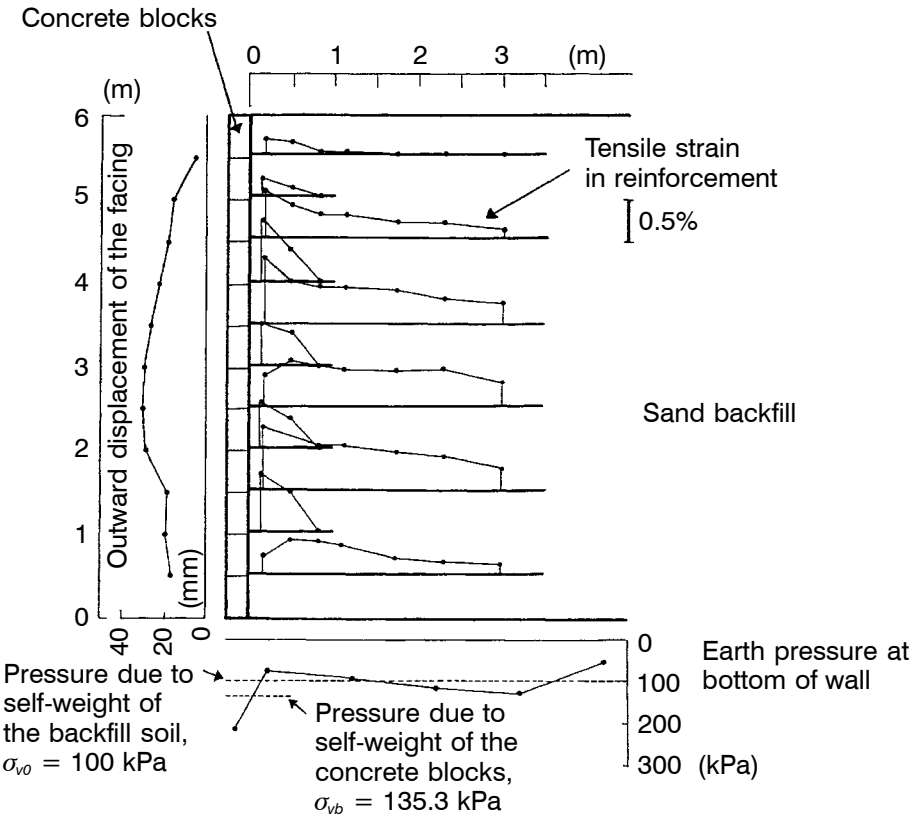

Figure 6. Behavior of a large-scale GRS-RW laboratory model wall (Tajiri et al. 1996).

wall was constructed on a rigid concrete floor. A concrete block facing was constructed concurrently with backfilling and compaction of a cohesionless soil reinforced with alternating long and short geogrid layers having a tensile rupture strength, T_R = 56.8 kN/m. The distribution of the tensile force in the geogrid layers is similar to the distributions A1 and A2 in Figure 5b. This is due to the rigidity of the facing.

The use of a FHR facing is more effective for increasing wall stability and reducing wall deformation than using a relatively flexible facing such as discrete panel facing, or a wrap-around facing (Tatsuoka et al. 1989b; Tatsuoka et al. 1991, 1992). Tatsuoka (1993) classifies different types of walls based on facing rigidity and discusses the contribution to wall stability.

In the current design method for GRS-RW systems, a FHR facing is designed to support the active earth pressure developed in an unreinforced backfill (Horii et al. 1994). However, the internal moment and the shear forces in the facing, the overturning moment, and the sliding force activated at the bottom of the facing can be very small because a FHR facing behaves as a continuous beam supported by a number of reinforcement layers with a very short vertical spacing (i.e. 300 mm) (Figure 4c). Therefore, the

facing can be very thin and the required amount of steel-reinforcement in the facing is minimal (Horii et al. 1994). The minimum facing thickness specified for a GRS-RW is 300 mm, which is based on constructability considerations. This thickness is typically larger than that based on structural requirements.

When the foundation subsoil is not very stiff, a conventional reinforced concrete (RC) cantilever retaining wall is typically supported on a pile foundation to prevent unacceptable wall displacement during construction and after wall completion (Figure 7a). Figure 8 shows an experimental 5 m high cantilever RC wall constructed directly on an intact layer of volcanic ash clay (Kanto loam) at the Chiba Experimental Station, University of Tokyo. The backfill was a nearly fully saturated soil obtained from a

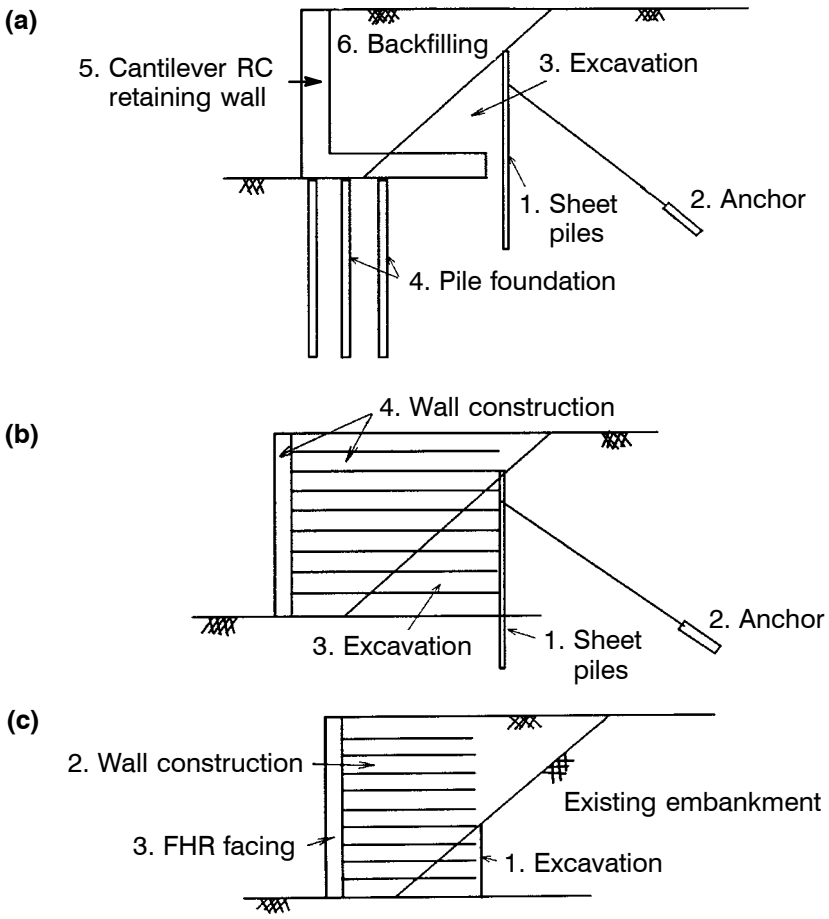

Figure 7. Comparison of different retaining wall construction procedures for reconstructing an existing slope: (a) a conventional RC cantilever reinforced wall; (b) a reinforced soil retaining wall with relatively long reinforcement; (c) a reinforced soil retaining wall with relatively short reinforcement and a FHR facing.

Note: Numbers refer to construction stage.

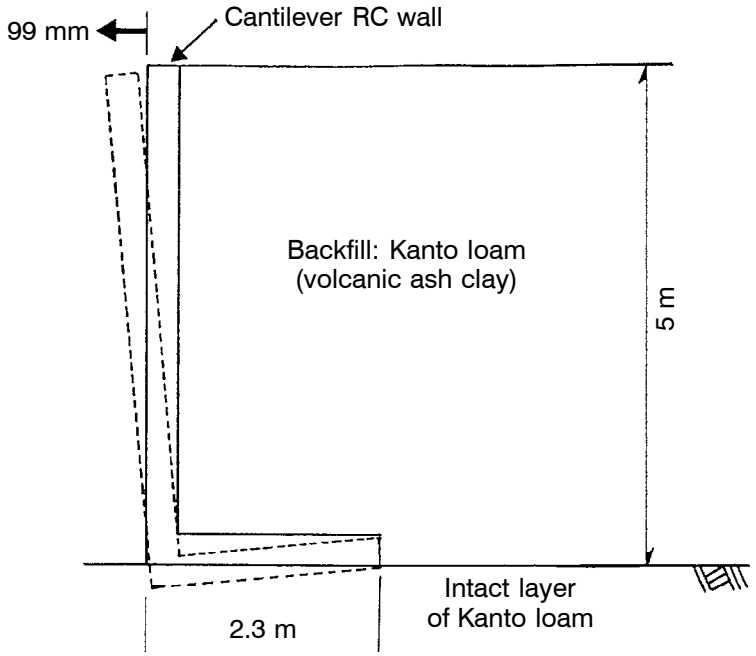

Figure 8. The experimental 5 m high cantilever RC wall at the Chiba Experimental Station, Institute of Industrial Science (IIS), University of Tokyo.

nearby deposit of Kanto loam. This soil, under intact conditions, is stable due to slight cementation, but it becomes very soft after remolding due to a high natural water content (approximately 100 to 120%) and a high degree of saturation (85 to 90%). The wall displaced outward by approximately 100 mm at the top of the wall face within six months after the commencement of backfilling.

2.2 Advantages of Staged Construction Procedures

It has been advocated that a GRS-RW with a flexible or deformable facing can accommodate the deformation of the backfill and the underlying subsoil layer. However, it is also desirable that a retaining wall be rigid and stable. This contradiction can be resolved by using the staged construction method and a FHR facing (Figure 1), that is:

- By using the staged construction method, potential damage to the connections between the facing and the reinforcement due to settlement of the backfill relative to the rigid facing is avoided.
- In the staged construction procedure, good compaction of the backfill adjacent to the back of the facing can be achieved by allowing relatively large outward lateral displacements to occur at the temporary wall face. Accordingly, sufficiently large tensile strains can be developed in the reinforcement. On the other hand, when a discrete panel, or a full-height panel facing is constructed prior to soil compaction, the soil adjacent to the back of the facing cannot be sufficiently compacted without a large earth

pressure on the facing, associated excessive lateral outward displacement of the facing, and damage to the connection between the reinforcement and the back of the facing. Accordingly, sufficiently large tensile strains cannot be mobilized during backfilling.

- When a full-height panel facing is propped during backfilling, uncontrollable outward displacement of the facing may occur upon removal of the prop. On the other hand, when unpropped discrete rigid panels are erected while the backfill is compacted, it may be difficult to ensure a good final facing alignment and post-construction displacement of the facing may continue (Tatsuoka et al. 1994). For the staged construction procedure with a cast-in-place FHR facing, the major portion of the potential deformation of the backfill and the subsoil layer takes place before facing construction, and hence good alignment of the facing is possible. In addition, a pile foundation used to support the facing is not necessary, mainly because the facing is laterally supported with many reinforcement layers, and therefore large moment and shear forces are not mobilized at the bottom of the facing (i.e. a self-supported structure; Figure 4c). Particularly, in the staged construction method, the facing is free from the effects of the downward vertical force caused by the reinforcement layers that settle relative to the facing during and after the compaction of the backfill.

It is noted that for staged construction procedures, the wall should be stable for a period of time before a FHR facing is cast in place. It has been confirmed by the full-scale behavior of many walls that a wall without a FHR facing (i.e. before subjecting it to a live load) is very stable, although some deformation of the wall may occur. The authors consider that the use of gravel-filled bags at the shoulder of each soil layer (Figure 1) with a relatively small vertical spacing of reinforcement layers (i.e. 300 mm) contributes greatly to the stability of a wall on a temporary basis.

A good connection between the facing and the backfill is essential for a stable completed GRS-RW. Because a stack of gravel-filled bags placed at the wall face has a very high drainage capacity, excess water from the concrete mix used to form the facing can drain through the bags (Figure 9). Thus, the formation of a weak and thin vertical concrete layer due to the accumulation of water along the back of the facing is effectively avoided. Furthermore, it has been observed that some fresh concrete penetrates the surface zone of the gravel-filled bags, and likely increases the contact strength between the concrete facing and the bags. The strength of the connection between the facing and the gravel-filled bags was determined from tensile load tests using a large test apparatus. It was found that the weakest section of the structure is not the connection between the concrete facing and the bags, but the geosynthetic wrapping around the bags (i.e. the geosynthetic) ruptured first. In addition, for prototype GRS-RWs, 13 mm diameter steel bars are typically placed at vertical and lateral spacings of 600 mm and are extended into the concrete facing (Figure 9) and connected to the steel reinforcement framework. This arrangement ensures an integral connection between the facing and the backfill.

2.3 Full-Height Rigid (FHR) Facing

The use of a FHR facing has the following additional advantages:

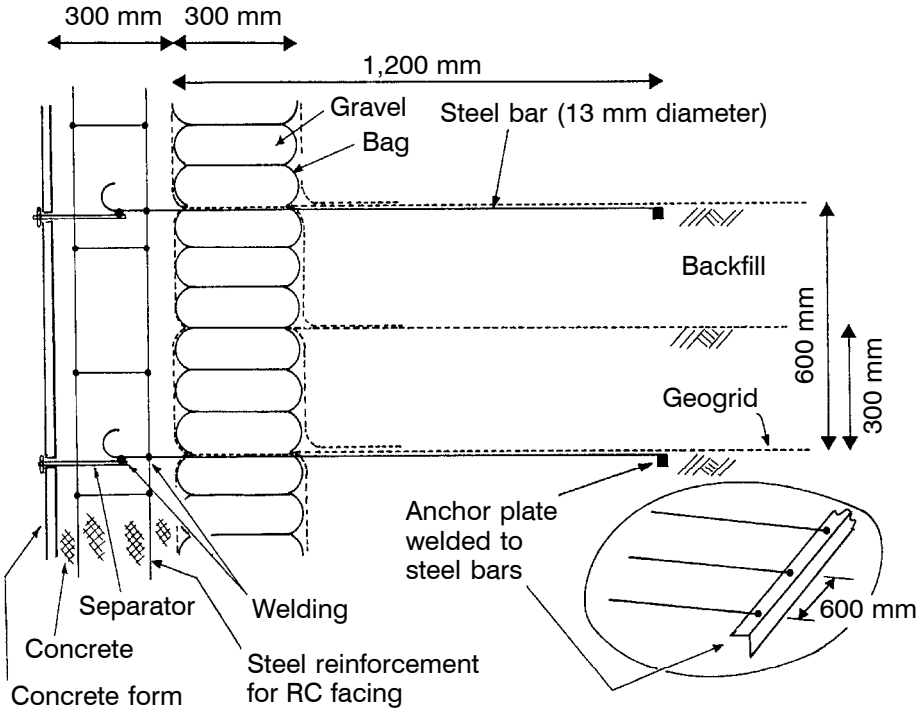

Figure 9. GRS-RW facing construction (not to scale).

- No major reinforced-soil retaining wall bridge abutments, including those with Terre Armée walls, had been constructed in Japan before the construction of a number of GRS bridge abutments with FHR facings (17 GRS bridge abutments were constructed prior to April 1997). These include three abutments for railways on the Seibu Line in Tokyo (Figure 10). During peak commute times, passenger trains cross the bridge every three minutes at high speed. The walls were constructed directly on a Kanto Loam soil deposit without using a pile foundation; the Kanto Loam is similar to the soil supporting the experimental cantilever RC retaining wall shown in Figure 8. No problems caused by settlement of the bridge girder due to the train load have been reported for these abutments. The use of a FHR facing made the construction of these GRS bridge abutments feasible. In particular, a GRS-RW with a FHR facing can effectively resist the seismic generated lateral loads of a bridge girder. This was confirmed for the Seibu Line walls by applying a lateral outward force up to 98 kN to a RC block denoted by the letter A in Figure 10a. Figure 11 shows the relationships between the lateral wall displacement at the facing at two levels, denoted as U and L, and the lateral load applied to a RC block to support the bridge girder. The lateral movement at the top of the facing was only 0.9 mm for this relatively large load. It may be noted that the displacement at level L was approximately one-half of the displacement observed at level U. This result demonstrates that the entire facing, sup-

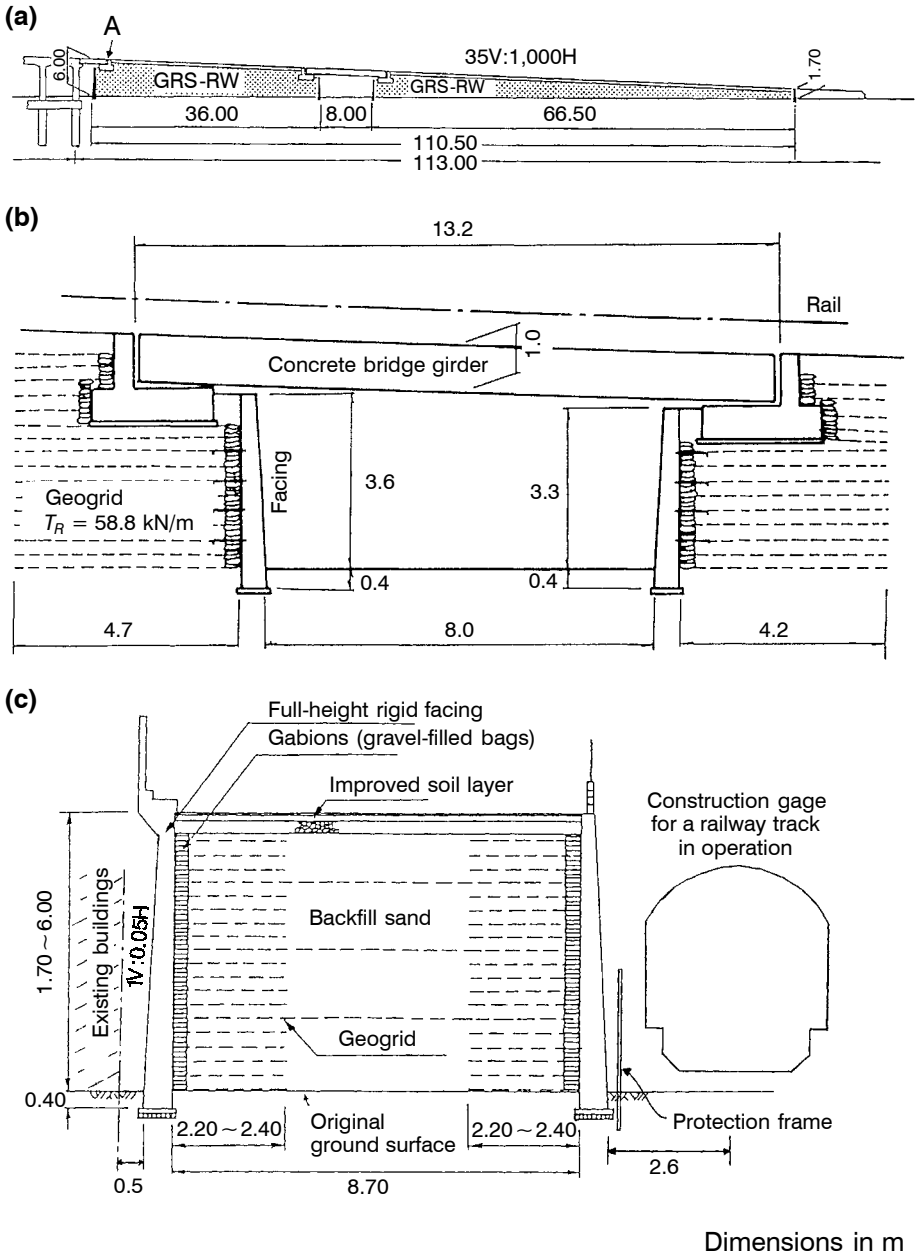

Figure 10. An abutment constructed as part of a GRS-RW system for the Seibu Line in Tokyo (Location 42, Figure 3): (a) general longitudinal section; (b) longitudinal section of the bridge abutment; (c) detailed cross section of the bridge abutment.

(d)

(e)

Figure 10 continued. (d) completed structure; (e) crest of the structure.

ported by all of the reinforcement layers, resisted the lateral load applied to the crest of the wall.

- This case is also noteworthy because of the restricted construction space. The space between the wall face and the trains is only 0.8 m wide, and the distance between the wall face and the existing buildings is only 0.5 m wide (Figure 10c). The facings were cast in place using concrete forms supported by steel bars anchored in the backfill soil without external support (Figure 9).
- Laboratory tests (Tatsuoka et al. 1989b) and full-scale loading tests (Tateyama et al. 1994a; Tamura et al. 1994) have shown that a GRS-RW with a FHR facing can support very large vertical and lateral loads acting at and immediately behind the crest of the wall without exhibiting noticeable deformation (as explained above). Therefore, in many cases, FHR facings have been used to directly support other types of structures (Figure 12a). When deformable facings are used, very complicated and expensive measures must be taken to support the same structure. For example, a RC block is required to support the noise barrier fence structure in Figure 12b (Tatsuoka et al. 1994).

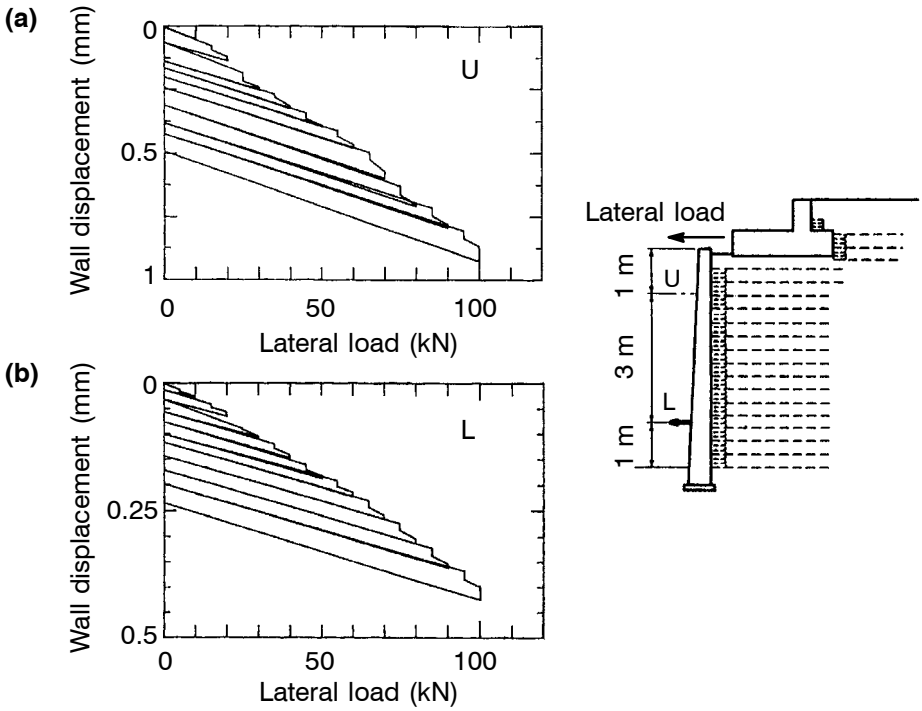

Figure 11. Relationships between the outward lateral displacement at the facing and the lateral load applied to the RC block to support the bridge girder (Seibu Line): (a) wall displacement at the upper wall location; (b) wall displacement at the lower wall location.

- A FHR facing contributes to the durability and aesthetics of the wall face when compared to a wrap-around wall face of a GRS-RW. For walls constructed in urban areas, the facings are often formed to give a stacked stone appearance at the face.
- It has been a major objective of many engineers to minimize the length of reinforcement when space is limited. When relatively long reinforcement is used (e.g. Figure 7b), sheet piles and anchors may be required to ensure the stability of the existing embankment during excavation. This may increase the cost of constructing the reinforced soil retaining wall. Note that relatively long metal strips must be used so as to ensure a sufficiently large reinforcement pull-out capacity that is comparable to the tensile rupture capacity of the metal. On the other hand, when the reinforcement is shorter (Figure 7c), slope excavation can be minimized without using sheet piles and anchors, which may result in a large cost reduction. The allowable reinforcement length can be made shorter by the use of not only planar reinforcement (i.e. geosynthetic sheets), but also a FHR facing. This means that, when compared to metal strips, planar polymeric reinforcement (e.g. geogrid) has a much shorter required anchorage length (typically 300 mm) to mobilize an anchorage capacity, T_{anchor} , that is equivalent to the tensile rupture capacity, T_R (Figure 5a). However, the use of shorter reinforcement may cause larger outward shear deformations of the wall (Jewell 1990). The use of a FHR facing causes the reinforced zone to behave as a monolith, which

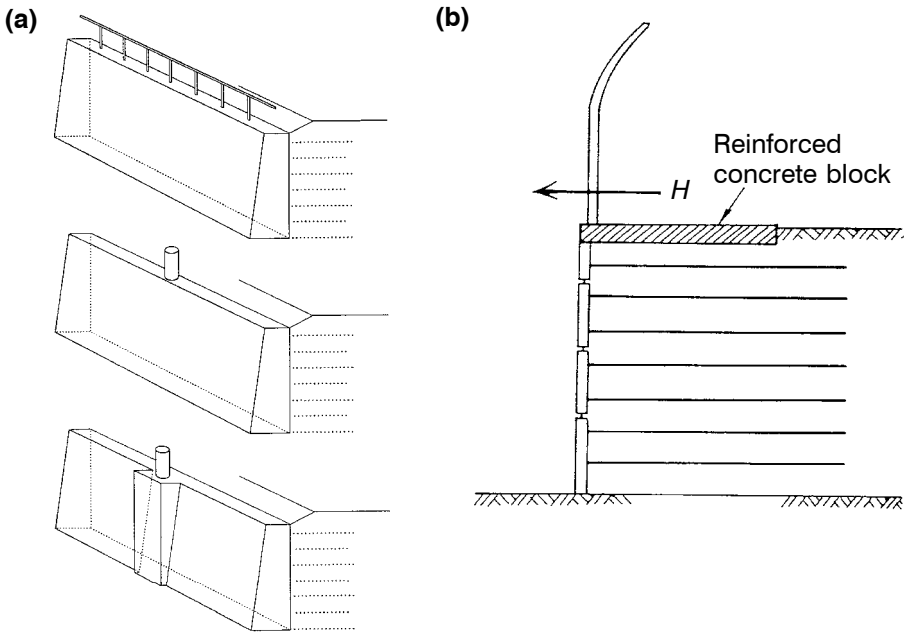

Figure 12. Reinforced soil retaining walls using different types of facing: (a) examples of structures constructed directly on a FHR facing; (b) deformable panel facing wall with a reinforced concrete block used to support a noise barrier fence (Tatsuoka et al. 1994).
Note: H = horizontal noise barrier fence force.

increases the stability of a wall with a FHR facing and decreases the shear deformation of the wall. For the GRS-RW system, the allowable minimum length of the reinforcement is specified to be 35% of the wall height, or 1.5 m, whichever is the larger value. Note that, as the reinforcement becomes shorter, more load may be concentrated toward the bottom of the facing, particularly during an earthquake. Therefore, the influence of the bearing capacity of the subsoil beneath the facing on wall stability cannot be ignored. In addition, to prevent overturning failure of a GRS-RW, it may be necessary to use longer reinforcement layers at higher levels in the wall as shown in Figure 13. These factors are considered in current design methods for GRS-RWs (Horii et al. 1994).

Generally, the construction cost for a GRS-RW system with a FHR facing (Figure 1) is higher than the cost of conventional geosynthetic-reinforced soil retaining walls with flexible facings. It should be noted, however, that GRS-RWs with FHR facings are much more cost-effective than conventional retaining walls constructed as permanent significant structures and, in many cases, more cost-effective than conventional metal-reinforced soil retaining walls. The authors believe that the use of a FHR facing is one of the most significant reasons why the GRS-RW system with a FHR facing has been chosen by practicing engineers for many important permanent retaining walls and bridge abutments in Japan. Two typical recent case histories that demonstrate the cost-effectiveness of GRS-RWs with FHR facings are described in Sections 3 and 4. Other

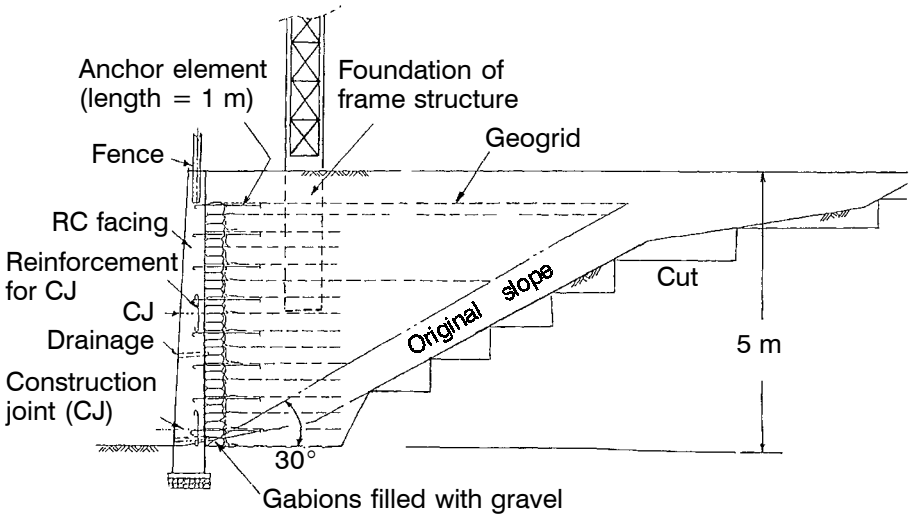

Figure 13. Typical cross section of the GRS-RW with a FHR facing for the Shinkan-sen (bullet train) train yard at Biwajima, Nagoya (Tatsuoka et al. 1992).

major projects and several case histories have been described by Tatsuoka et al. (1992), and by Tatsuoka and Leshchinsky (1994).

3 NAGANO WALL

3.1 General

The Nagano wall is 2 m high and approximately 2 km long (thick solid line in Figure 14a), and was constructed at a train yard for the Hokuriku Shinkansen (bullet train) in the northern section of Nagano City (Location 38, Figure 3). This wall is one of the best examples that demonstrates the advantages of the staged construction method. The wall was constructed from 1993 to 1996. Additional 100 m long GRS-RW sections with FHR facings and two 3.4 m high GRS bridge abutments with FHR facings were constructed commencing in 1995 for the approach fill to the train yard (Figure 14b). For these additional structures, a very soft clay layer beneath the approach fill was improved by cement-mixing in-place to avoid intolerably large settlements relative to the adjacent RC bridge abutment that is supported by a pile foundation.

3.2 Preloading and Settlement

For the walls at the train yard, the subsoil is a significantly thick deposit of very soft clay. Therefore, a preload fill was placed on the embankment behind the GRS-RWs before constructing the FHR facing. This resulted in a large amount of fill settlement (approximately 1 m) (Figures 14c and 14d). The initial wall height as constructed was 3 m to accommodate this large amount of settlement. It should be noted that no pile

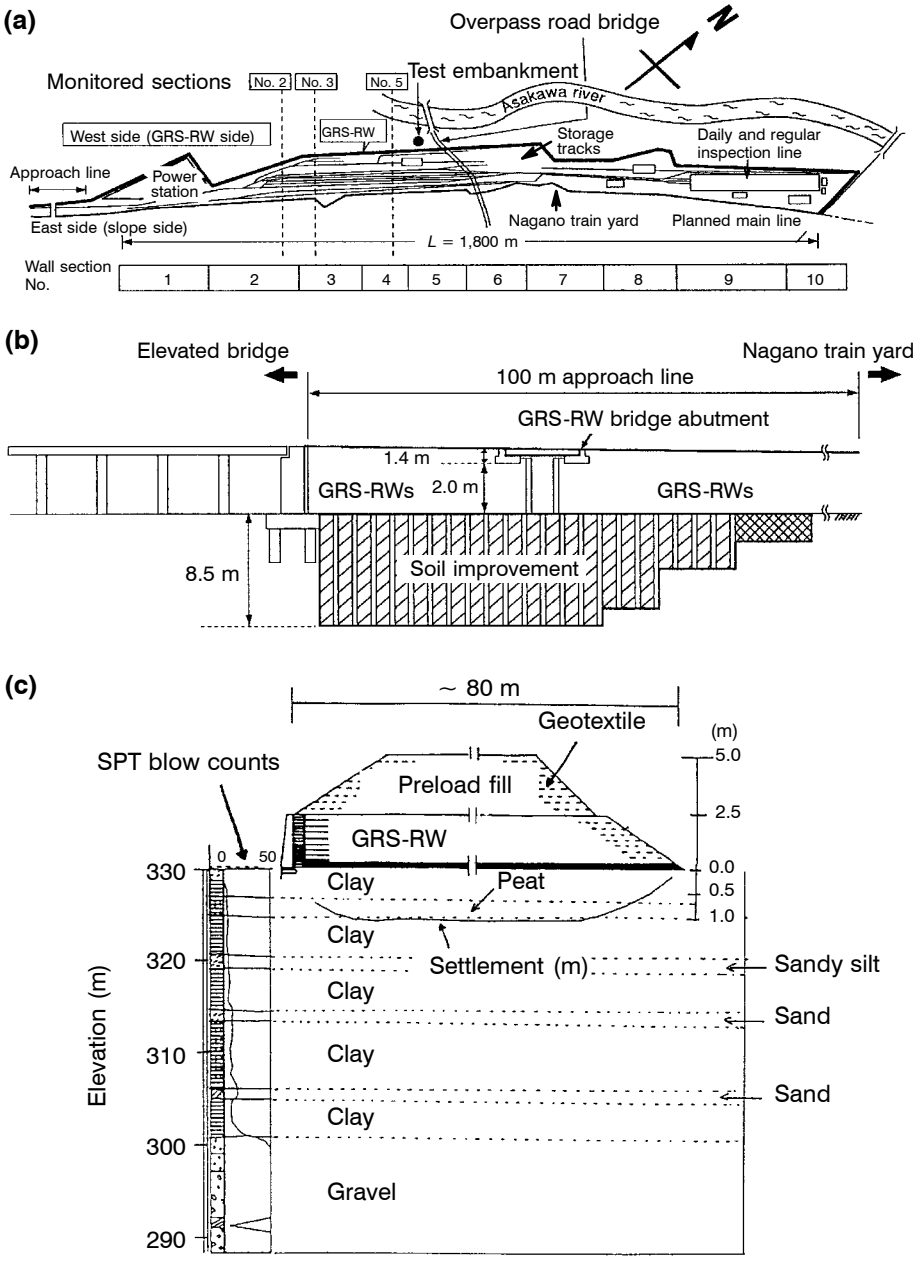

Figure 14. Nagano GRS-RW with a FHR facing for the Hokuriku Shinkansen (bullet train) north of Nagano City: (a) plan view of the train yard; (b) longitudinal section of the approach fill to the train yard; (c) typical cross section of an embankment with a GRS-RW in the train yard.

Note: SPT = standard penetration test.

(d)

(e)

(f)

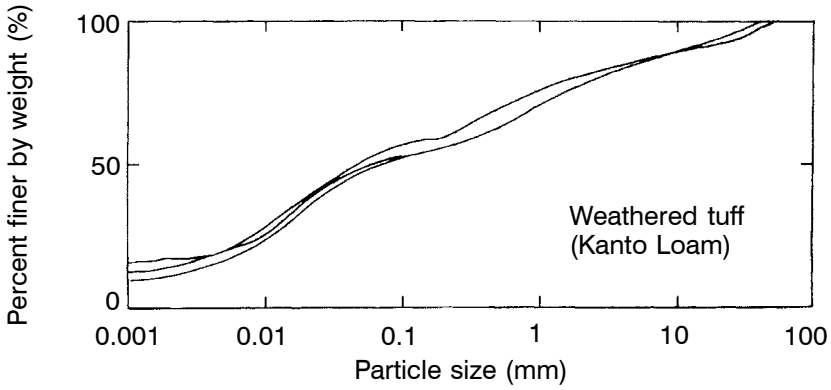

Figure 14 continued. (d) Nagano wall during preloading; (e) cast-in-place construction of the FHR facing after the preload fill was removed; (f) typical gradation curves for the Kanto Loam backfill.

foundations were used, which would have been necessary if conventional cantilever RC retaining walls were constructed. A FHR facing was cast in place during the summer of 1996, approximately one year after a six month preloading period (Figure 14e).

3.3 Clay Backfill

The Nagano wall is an important case because it was the first time a nearly fully saturated on-site clay (highly weathered tuff) was used as backfill (Figure 14f). The decision to use the clay was based on the good performance of a series of full-height GRS-RWs with a backfill of nearly fully saturated volcanic ash clay (Kanto Loam) (Tatsuoka et al. 1986, 1987; Tatsuoka and Yamauchi 1987; Tatsuoka 1993; Yamauchi et al. 1987; Ling et al. 1995). This soil became a nearly saturated soft clay after compaction with an average water content of approximately 30% and a degree of saturation of 70% . The backfill soil was reinforced with a composite nonwoven-woven geotextile with a rupture strength, T_R = 35.3 kN/m at a failure tensile strain of 7%, and a stiffness, J = 490 kN/m at an elongation of 5%.

The use of a low-quality on-site soil as the backfill contributes to a large cost reduction as compared to using an expensive imported cohesionless soil and disposing of the low-quality excavated soil. The results of small-scale laboratory model tests (Ling and Tatsuoka 1994) showed that saturated clay can be effectively reinforced with a geotextile composite by consolidating the soil anisotropically under operational field conditions. This result is consistent with the good performance of the full-scale walls mentioned above.

3.4 Comparison and Summary

At this site, the importance of the FHR facing was reconfirmed by comparing the behavior of two experimental GRS-RWs with and without a FHR facing after the construction of fill on top of the walls. The deformation of the walls without a FHR facing was noticeably larger than that of the wall with a FHR facing (Tatsuoka et al. 1997a).

The success of the Nagano wall demonstrates that most types of on-site soils including those of “inferior” quality (e.g. sandy soils containing a large amount of fines, or nearly saturated fine grained soils) can be used for the backfill soil of a GRS-RW system. This is a significant advantage over steel-reinforced soil retaining wall systems that are restricted to clean sand or gravel backfill soils (Zornberg and Mitchell 1994; Mitchell and Zornberg 1995).

4 RECONSTRUCTION OF RAILWAY EMBANKMENTS IN KYUSHU

4.1 1989 Damage and Reconstruction

In the Mount Aso area in Kyushu Island, a series of railway embankments on the Hohi Line located in narrow valleys were destroyed during heavy rainfall on 2 July 1989 (Figure 15). The damage was caused by flood water that was trapped upstream of the embankment due to the clogging of a drain pipe crossing each embankment. Six entire sections of the embankment were reconstructed (Figure 16). To reduce the amount of earthwork, an approximately vertical GRS-RW with a FHR facing was constructed at the downstream toe of each embankment, and the slope was reinforced with geogrid (Tatsuoka et al. 1992). This remedial work is characterized by very large embankment heights and a large diameter corrugated steel drain pipe installed in each embankment.

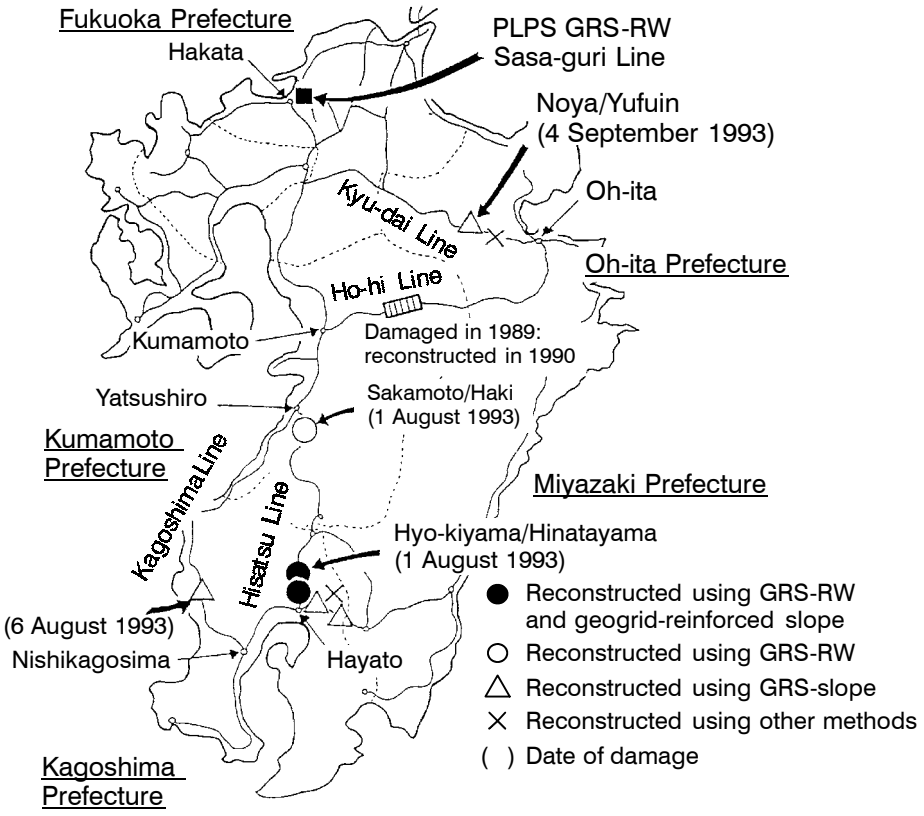

Figure 15. Location of railway embankments seriously damaged by heavy rainfalls in 1989 and 1993, and the location of the first PLPS GRS bridge pier (Sasa-guri Line).

4.2 1993 Damage and Reconstruction

From June to September 1993, many railway embankment sections in central and southern Kyushu at the sites highlighted in Figure 15 were seriously damaged or destroyed by a series of heavy rainfalls. The scale of damage was significantly greater than the damage incurred in 1989. The total precipitation during these months in Kagoshima and Miyazaki Prefectures amounted to approximately 3,000 mm. By November 1993, damaged embankment sections denoted by solid circles in Figure 15 were reconstructed using a method similar to that used in 1989 (Figure 17). The total volume of the damaged embankments that were reconstructed was 18,700 m^3. The original fill material for the wall (at the Hyo-kiyama/Hinatayama site) was a pumice called Shirasu, which was washed away from the embankment toe by a flood. The total volume of crushed stone gravel used for the reconstruction was 8,640 m^3. The reconstruction method was adopted based on the successful previous construction on the Ho-hi Line (i.e. it had a low construction cost, relatively short construction period and required relatively light

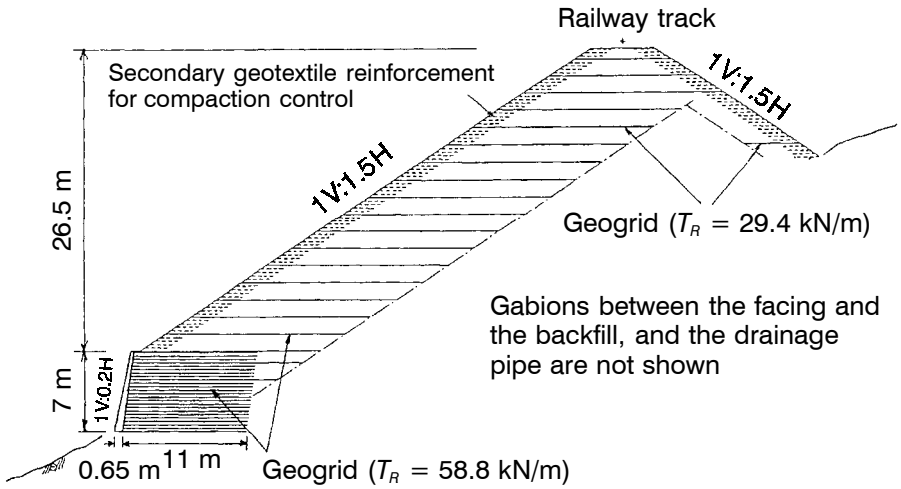

Figure 16. Typical cross section of the reconstructed railway embankment at the Mount Aso site (the Ho-hi Line, Location 8, Figure 3).

construction equipment). The last two factors are particularly important because rapid remedial work was required, and most of the damaged embankments were located in remote mountainous areas.

At the site denoted by a hollow circle in Figure 15 (Sakamoto/Haki site), a conventional masonry retaining wall was completely destroyed for a length of approximately 59 m by flooding of the adjacent river. The wall was reconstructed using the GRS-RW system (Figure 18). At several other sites denoted by hollow triangles in Figure 15, the slopes of the damaged embankments (total soil volume of 7,700 m^3) were reconstructed using geosynthetic reinforcement layers. The other sections comprising a total soil volume of 3,600 m^3 were reconstructed without using geosynthetic reinforcement.

5 DEFORMATION OF REINFORCED SOIL RETAINING WALLS

5.1 Creep Deformation

It has been claimed that most currently available geosynthetic reinforcing materials are too extensible and exhibit larger creep elongation than steel strip reinforcement (e.g. Schlosser et al. 1994). In most cases, however, the deformation of a wall during construction is not a serious problem. Rather, creep deformation of the wall by dead, live, and/or seismic loads while in service should be smaller than the specified allowable limit. There are no cases of GRS-RWs with FHR facings that exhibited noticeable long-term creep deformation despite the use of so called "extensible" reinforcement (i.e. polymer geogrid). Probable reasons for this fact include the following:

1. GRS-RWs with FHR facings have a sufficient margin of safety resulting from the conservatism exercised at several design stages. In particular, GRS-RWs are de-

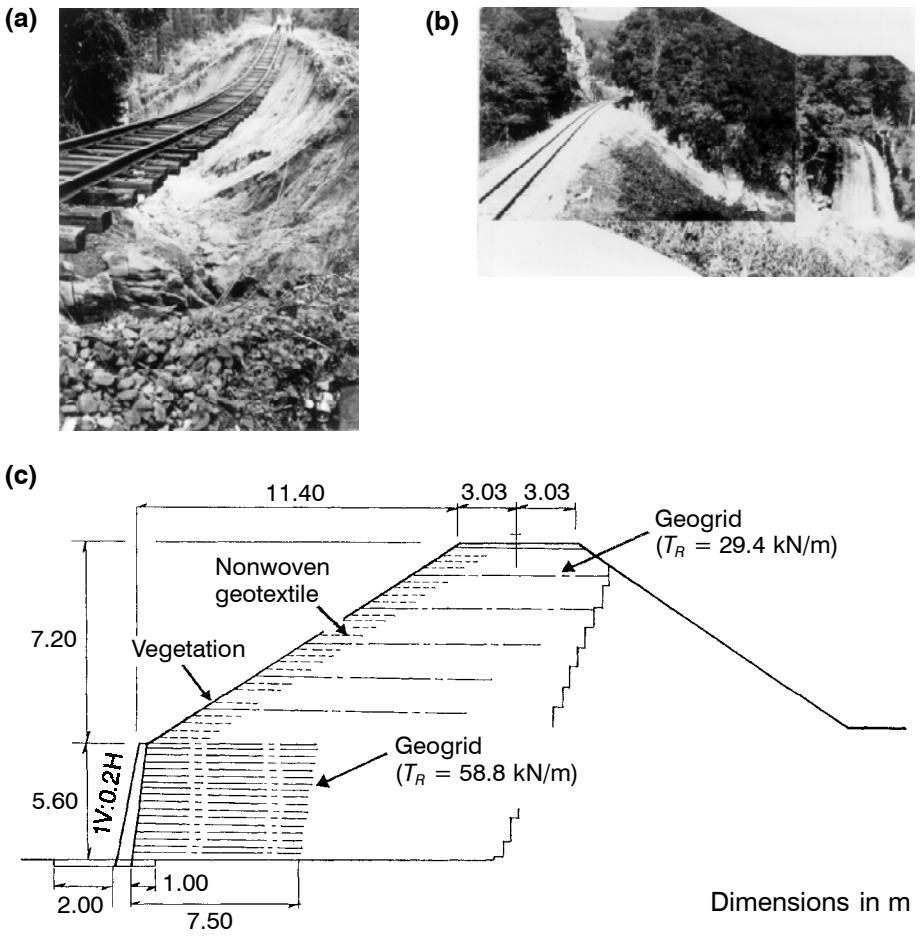

Figure 17. Railway embankment damage and reconstruction in 1993 at Hyo-kiyama/Hinatayama site, the Hisatsu Line (Location 35, Figure 3): (a) damaged embankment; (b) reconstructed embankment; (c) typical cross section of a reconstructed embankment.

signed for seismic loading using pseudo-static limit equilibrium stability analysis methods with a horizontal seismic coefficient, k_h = 0.2. This results in sufficiently large factors of safety for GRS-RWs under ordinary load conditions.

2. In a reinforced soil retaining wall with a deformable facing, deformation will occur mainly at the wall face and in the backfill immediately behind the wall face. The use of a FHR facing can effectively prevent this deformation.

Creep deformation of GRS-RWs with FHR facings is discussed in more detail by Tatsuoka and Uchimura (1997b).

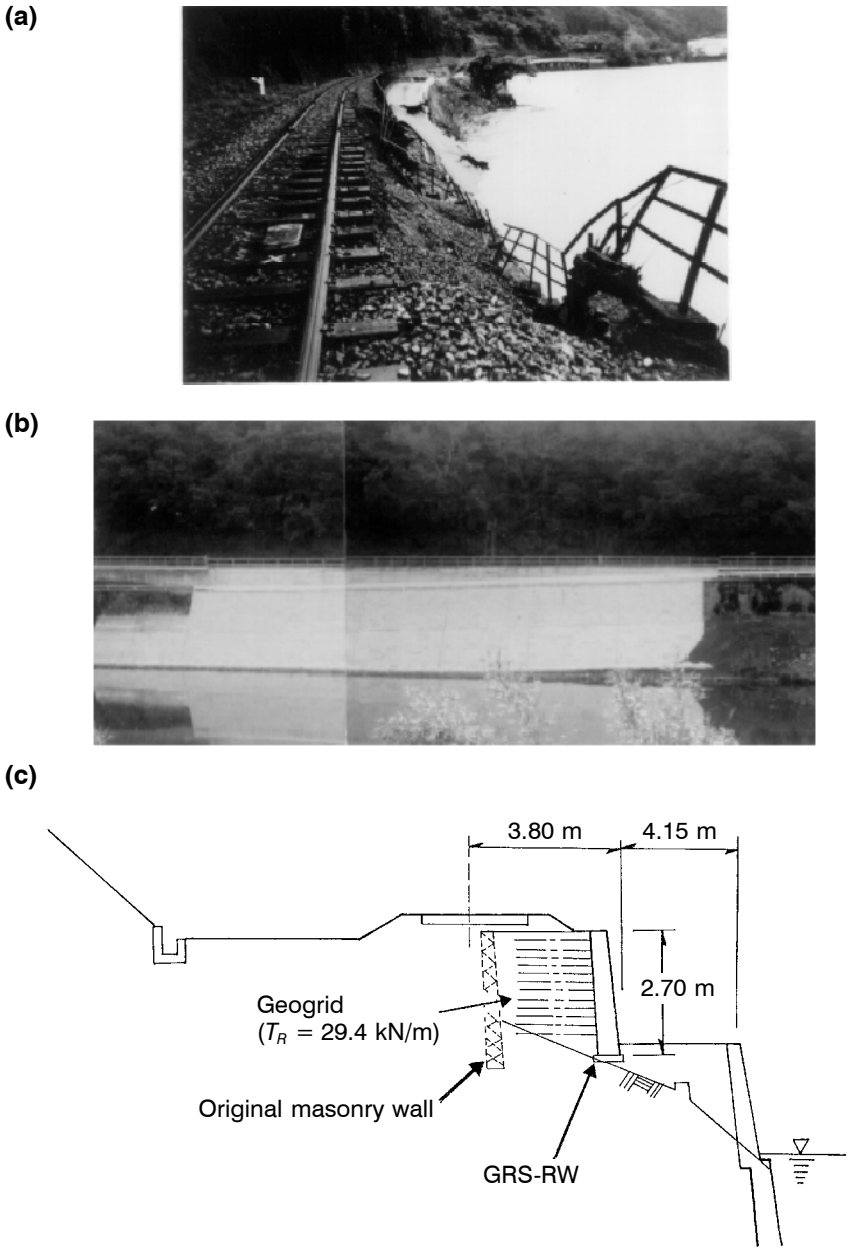

Figure 18. Railway embankment damages and reconstruction in 1993 at the Sakamoto/Haki site on the Hisatsu Line (Location 35, Figure 3): (a) damaged embankment; (b) reconstructed embankment; (c) typical cross section of the reconstructed soil retaining wall.

5.2 Preloaded and Prestressed (PLPS) GRS-RWs

5.2.1 *Background*

The longest bridge girder supported by GRS bridge abutments in Japan with FHR facings is 13.2 m (Figure 10b). To support a longer and heavier bridge girder, the GRS bridge abutments should be stiffer than those constructed thus far. It should be noted that since reinforcement is effective only after the surrounding soil expands sufficiently in the horizontal direction, it is very difficult to substantially increase the vertical stiffness of a reinforced soil mass against a vertical working load even by using densely spaced, long, and very stiff reinforcement (Huang and Tatsuoka 1990).

5.2.2 *Working Principles*

Tatsuoka et al. (1996b, 1996c, 1997b) and Uchimura et al. (1996) proposed a new construction method to produce a significantly stiff reinforced soil by preloading and prestressing (PLPS) (Figure 19). In this paper, for the backfill soil, preloading (PL) is defined as the application of a vertical load that is larger than the final and current load

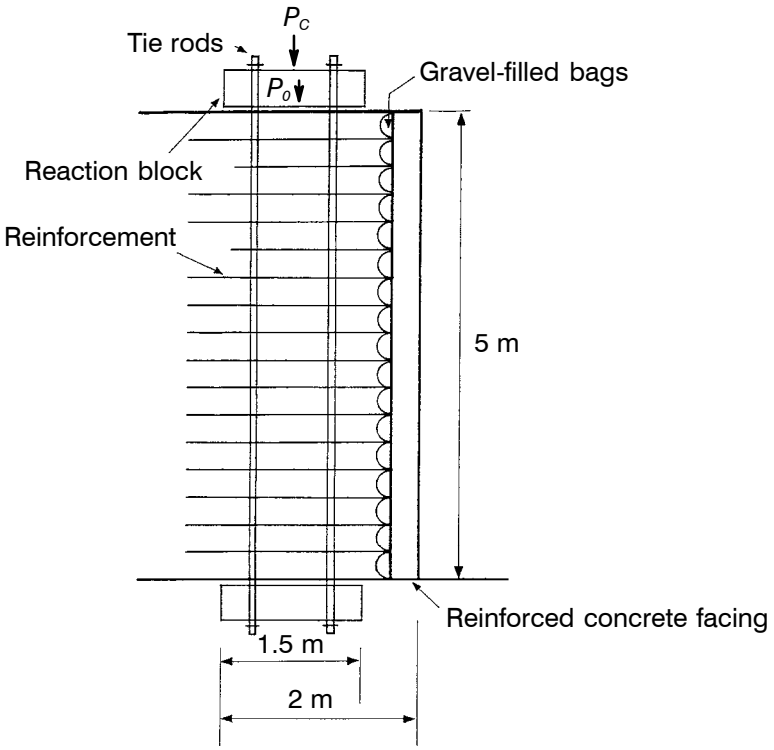

Figure 19. A typical PLPS GRS retaining wall (tie rods act as a compressive structural component against the external vertical load, P_C).

on the crest of the backfill, while prestressing (PS) corresponds to a non-zero load at the time of external load application (see Figure 20).

For this method, a GRS-RW is constructed using a modified staged construction method (Figure 1), with a pair of lower and upper reaction blocks connected by four tie rods, or with only a top reaction block connected to tie rods that are anchored in the ground below the backfill. Before a FHR facing is cast in place, the wall is preloaded and prestressed as follows:

1. A sufficiently large preload is applied using hydraulic jacks that are mounted at the top ends of the tie rods. A relatively large preload can be applied without causing failure of the backfill because the backfill soil is reinforced. Since preloading and subsequent unloading bring the backfill to an unloaded condition, the wall deforms nearly elastically when the external vertical load, P_C , is applied on top of the reaction block (Figure 21).

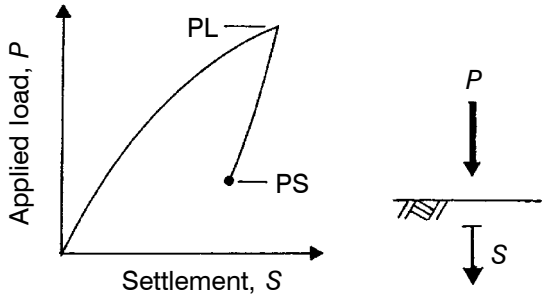

Figure 20. Definition of preload (PL) and prestress (PS) ($P = P_C + P_0$).

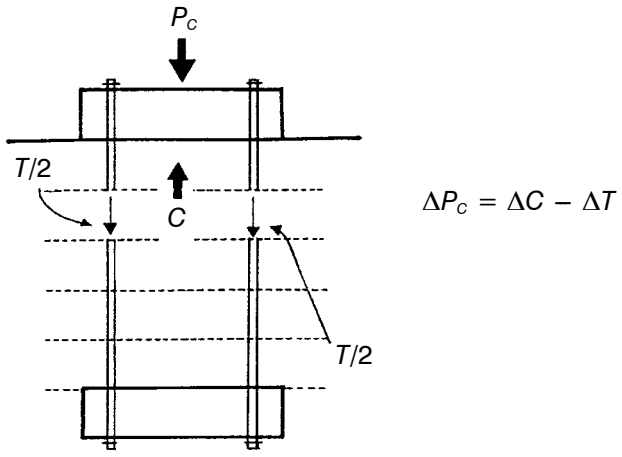

Figure 21. Load equilibrium (defining P_C , T and C).
Notes: C = compressive load applied to the top of the backfill; T = tension in the rods; P_C = external vertical load.

2. After unloading from the preloaded state to a certain load level, the top ends of the tie rods are fixed to the upper reaction RC block and the hydraulic jacks are removed. The tension, *T*, remaining in the tie rods functions as the "prestress", which is balanced by the corresponding compressive force *C* acting on top of the backfill (Figure 21). There are four additional reasons why a high prestress should be maintained to achieve a high performance of PLPS GRS-RWs.

   - First, the prestress maintains a large value of elastic stiffness in the backfill when compared to the value in the case without prestress. That is, as described previously (Tatsuoka et al. 1997b; Uchimura et al. 1996; Jiang et al. 1997), the Young's modulus, E_v, defined for a change in the major elastic principal strain in the vertical direction, ε_v^e, is proportional to $(\sigma_v)^m$ for most cohesionless soils where m is a constant; i.e. σ_v is the vertical normal stress, and $E_v = (\partial\sigma_v / \partial\varepsilon_v^e)$ in the rigorous mathematical expression. For most cohesionless soils, the value of m is approximately 0.5. In an extreme case with $\sigma_v = 0$, the value of E_V becomes zero even after a large preload (PL) has been applied.
   - Second, a rebound to zero load after preloading results in "soil swelling" (Figure 22a). The "swelling" behavior is due to: (i) a release of elastic energy stored in sections of the soil; and, (ii) a 90° rotation in the σ_1-direction.

     This swelling behavior is similar to that observed in one-dimensional compression tests on soils (i.e. oedometer tests). The 90° rotation is important particularly for preloaded reinforced soil. That is, the residual tensile force is introduced in the reinforcement by preloading and subsequent unloading to a zero load level. Then, the local stress condition in the soil could be such that the local lateral stress, $(\sigma_h)_{local}$, is larger than the local vertical stress, $(\sigma_v)_{local}$ (Figure 22b) in comparison to the compression stress condition with $(\sigma_v)_{local}$ larger than $(\sigma_h)_{local}$ during preloading. This change in stress conditions upon unloading to a zero load level causes a sudden

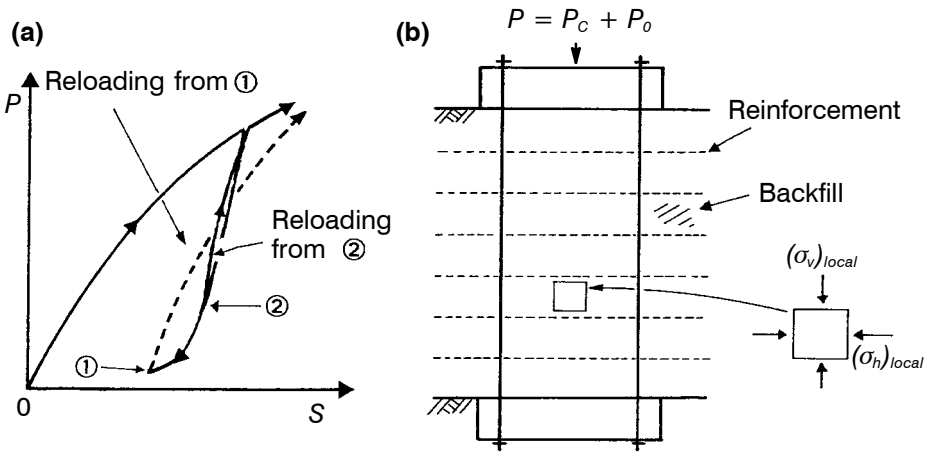

Figure 22. Preloading and prestressing the backfill soil: (a) swelling and the subsequent soft response of the backfill soil after preloading; (b) local stress conditions when the backfill is unloaded to a zero load level after preloading.

90° rotation in the direction of the principal stresses, which is known to damage the soil structure and reduce the tangential stiffness when reloaded. Due to the combined effects of these two factors, the soil stiffness upon reloading after preloading to a zero load level (Case 1 in Figure 22a) becomes much less than when unloaded to and reloaded from a non-zero load level (Case 2 in Figure 22a).

The above-mentioned behavior has been observed in the full-scale PLPS GRS bridge pier as described in Section 5.2.4 (Uchimura et al. 1996, 1997), and in a plane strain compression (PSC) test on geogrid reinforced Toyoura sand performed in the laboratory (Figure 23) (Tatsuoka and Uchimura 1997a). It may be seen in Figure 23 that a relatively large amount of swelling occurs when the soil is unloaded to near-zero load states, followed by a relatively softer response when subsequently

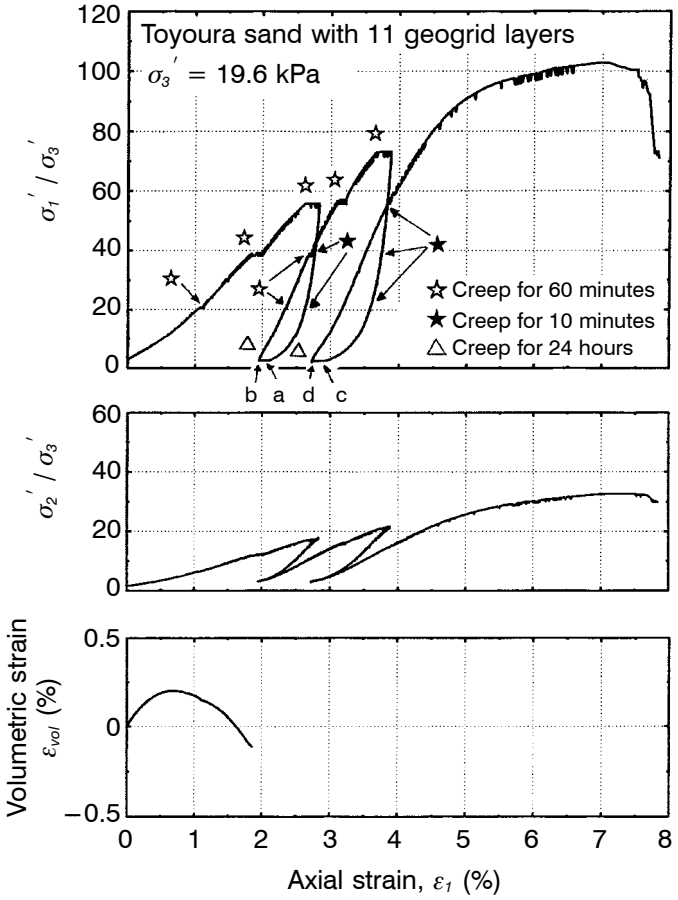

Figure 23. Results of a plane strain compression (PSC) test on reinforced Toyoura sand (specimen size = 214 mm × 244 mm × 570 mm high; void ratio = 0.609; vertical geogrid spacing = 52 mm) (Tatsuoka and Uchimura 1997a).

Notes: σ_1 and ε_1 are the average axial stress and strain, respectively.

reloaded. The decrease in the axial strain, ε_1, for a time duration of one day from Point a to Point b and from Point c to Point d is due to creep recovery of the soil caused mainly by the residual tensile force in the reinforcement.

- Third, for a PLPS GRS to achieve high seismic resistance, shear strain values in the backfill soil should be maintained as small as possible. In particular, shear strains, ε_γ, should be small (Figure 24). For this purpose, a high shear modulus, G, should be achieved, which can also be obtained under a high pressure (i.e. high σ_v).
- Lastly, to achieve an acceptable performance of a PLPS GRS when subjected to high seismic loads (i.e. the level II design seismic load used in Japan), the PLPS GRS should be very ductile (i.e. capable of not losing strength even after large deformations). Sufficient ductility can be expected for a very densely compacted backfill if a constant (or nearly constant) volume condition is achieved during seismic loading. Figure 25 illustrates the ductile behavior of a dense soil under a

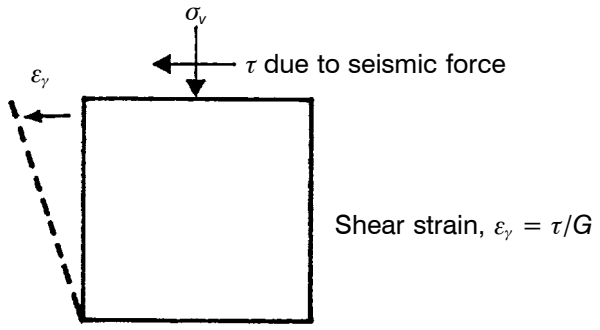

Figure 24. Definition of shear strain, ε_γ.

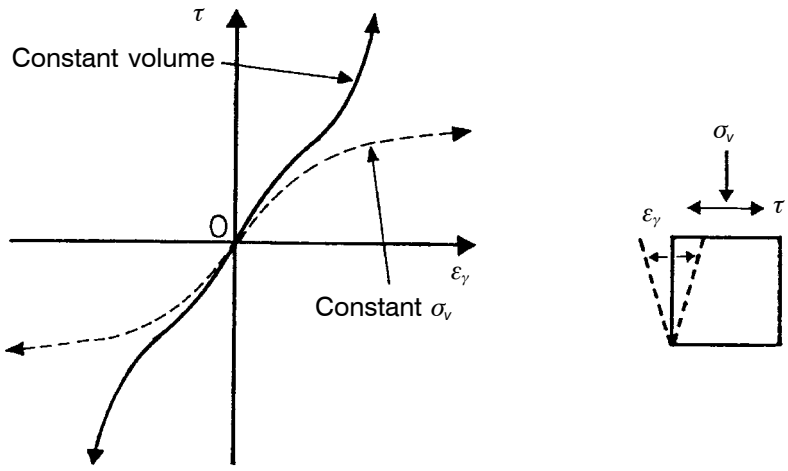

Figure 25. Constant volume versus constant normal stress, σ_v, behavior of a dense soil.

constant volume condition due to strong dilatancy, compared to the drained behavior. A PLPS GRS can deform under nearly constant volume conditions when the height of the backfill is kept constant, because the lateral tensile strains in the backfill are restrained by the reinforcement. A constant backfill height can be maintained by preventing the top reaction RC block from moving upwards relative to the tie rods. Figure 26 shows the behavior of dense sand under constant volume sim-

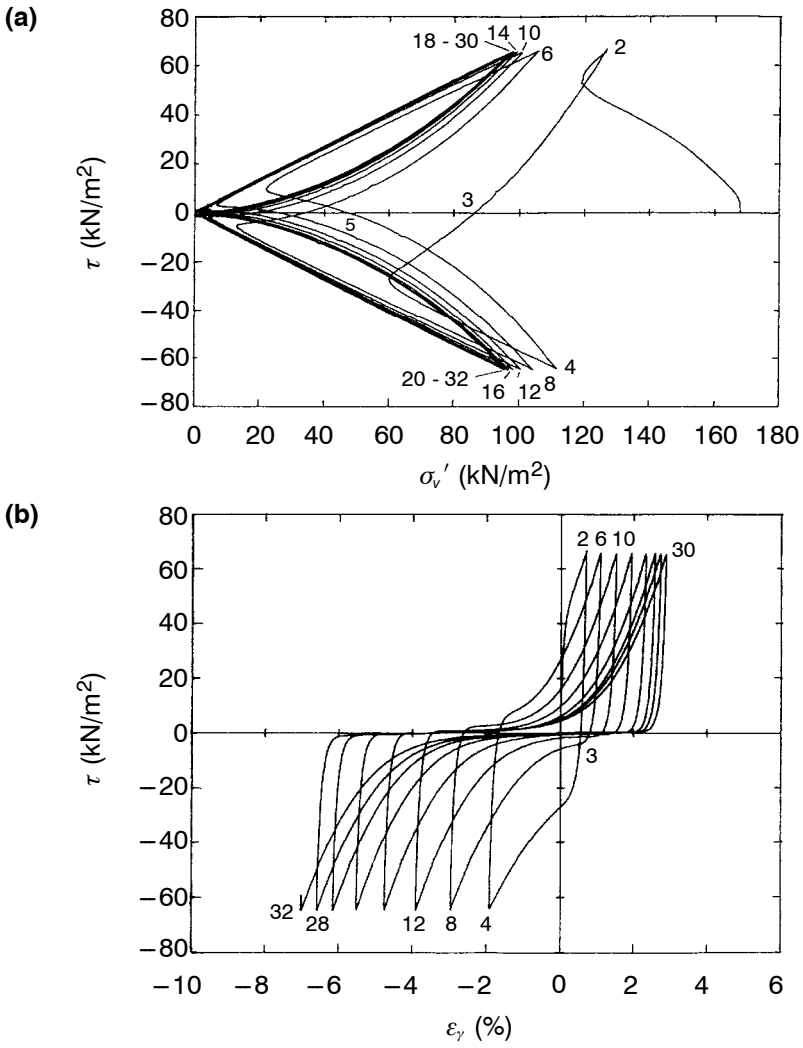

Figure 26. The behavior of a dense Toyoura sand (*e* = 0.680), under constant volume cyclic simple shear conditions: (a) shear stress and shear strain relationship; (b) effective stress path for a cyclic torsional simple shear test on an undrained specimen (Tatsuoka et al. 1989a).

ple shear conditions when subjected to cyclic shear stresses. Prestressed GRS-RWs are expected to behave in this manner when subjected to very high seismic loads.

For the above mentioned reasons, sufficiently large prestresses should be maintained while the wall is in service. A possible practical method to maintain a high backfill prestress for a long service life when subjected to continuous cyclic live loads is discussed in Section 5.2.4.

3. When the load, P_C, is applied to the top reaction block, the tension, T, in the tie rods decreases somewhat due to the compression of the backfill. The increase in the vertical load, C, on the top of the backfill due to the load P_C becomes smaller by the same amount, when compared to the increase in T for the case without prestress (Figure 21).
4. By preloading and subsequent unloading, prestress is also induced in the reinforcement members as a result of the interaction between the elasto-plastic properties of soil and the elastic properties of reinforcement ($(\sigma_h)_{local}$ in Figure 22b). This prestress can also contribute to maintaining wall integrity.

5.2.3 *Field Model Tests*

To validate the feasibility of the PLPS method, full-scale test walls were constructed in early 1995 at the Chiba Experiment Station, Institute of Industrial Science (IIS), University of Tokyo (Figure 27). The test sections were 4 m deep and were maintained under nearly plane strain conditions. A well-graded gravel composed of crushed sandstone was compacted to a dry unit weight, γ_d = 18.4 kN/m^3 with an average water content of 7.0%. The geogrid is made of polyvinyl alcohol (PVA) (with the trade mark name "Vinylon") and has a nominal tensile rupture strength, T_R = 73.5 kN/m. This type of geogrid is widely used in GRS-RW construction projects in Japan.

Commencing at the end of August 1995, test segments 3S, 3N and 3M, shown in Figure 27, were preloaded. For segment 3S, the first preload with an average contact pressure of 123 kPa was applied to the top reaction block (base area of 5.7 m^2) for approximately ten minutes (Figure 28a). For segment 3N (Figure 28b), creep deformation was permitted for 63 hours using a constant preload, during which the top block settled approximately 13 mm. For segment 3M, using a larger top reinforced concrete block base area of 2 m $\times$ 3.8 m = 7.6 m^2, stress relaxation was permitted for 22 hours after unloading from the first short preloading period (Figure 28c). Then, the second preload was applied and maintained at a constant level for 66 hours with the final creep settlement equal to approximately 7 mm.

The summary of the time histories of the contact pressure beneath the top reaction block are shown in Figure 29. Figure 30 shows the relationship between the average contact pressure and the average settlement of the top reinforced concrete block relative to the bottom reaction block in test segment 3M. The following trends in the behavior of the backfill may be noted with respect to Figures 29 and 30:

1. When a noticeable amount of creep deformation of the backfill was not permitted to occur during preloading (i.e. segments 3S and 3M after the first preloading), the rate of stress relaxation immediately after unloading was very high.

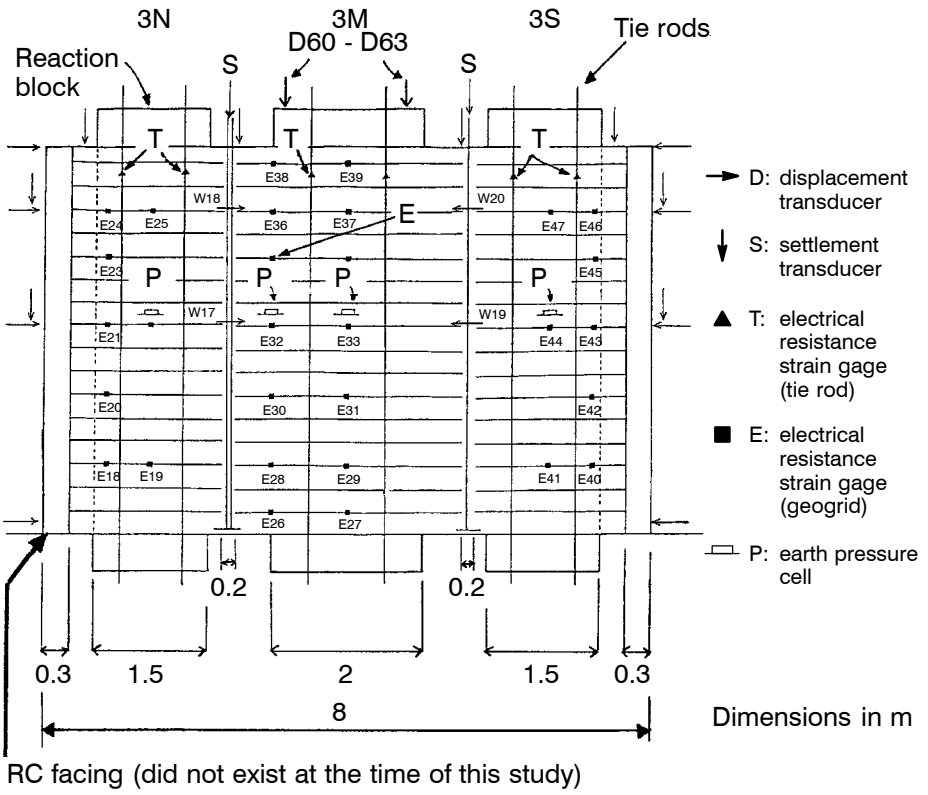

Figure 27. Cross section of the test wall divided into three PLPS GRS test segments (test wall was 5 m high, 4 m deep and 8 m wide).

2. By allowing some creep deformation of the backfill to occur during preloading (i.e. segments 3N and 3M after the second preloading), the rate of stress relaxation was noticeably lower.
3. The rate of stress relaxation increased suddenly due to heavy rainfall: 130 mm of precipitation caused by Typhoon No. 12 on 17 September 1995. Since the gravel had an initial water content of approximately 7.0% with 8.0% fines content, it appears that capillary suction was created during compaction, and that some of this capillary suction may have been lost by wetting.
4. When segment 3M was preloaded, a noticeable reduction in the tie rod tension in segments 3N and 3S occurred, which is likely due to the associated compression of the gravel backfill in these segments.
5. The relaxation rate in segment 3M after the second preloading period, and the relaxation rate in segments 3S and 3N after preloading segment 3M, significantly decreased. Subsequently, for more than eight months, the prestress only decreased slightly.

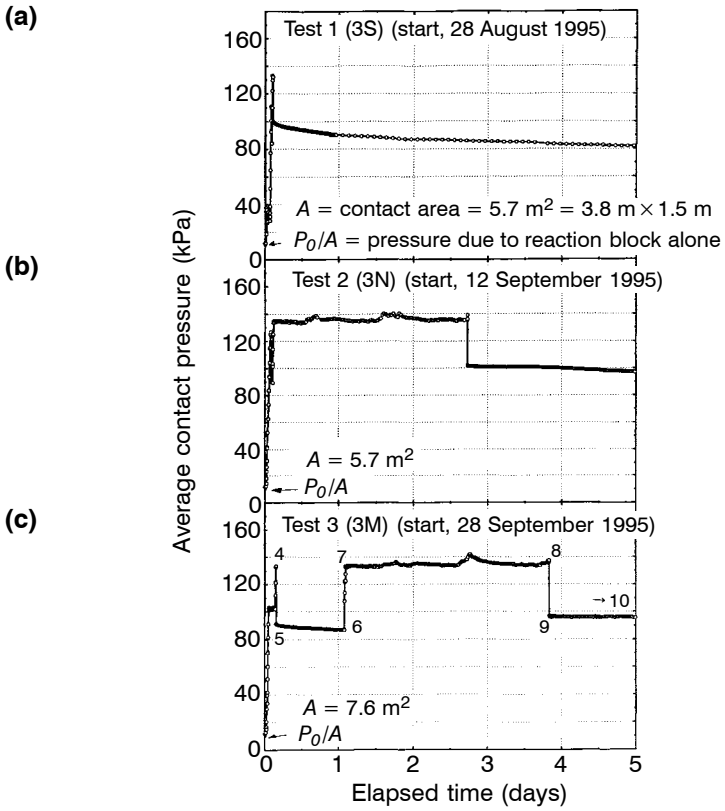

Figure 28. Time histories of the average contact pressure, $(P_0 + T)/A$, at the top RC block for three test sections: (a) 3S; (b) 3N; (c) 3M.

Notes: P_0 = weight of the top reaction RC block; T = tie rod tension.

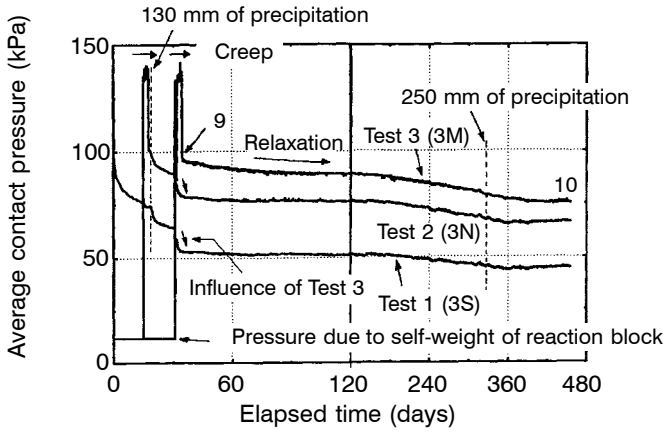

Figure 29. Summary of the time histories of the average contact pressure, $(P_0 + T)/A$, at the top RC block for the three PLPS GRS test segments.

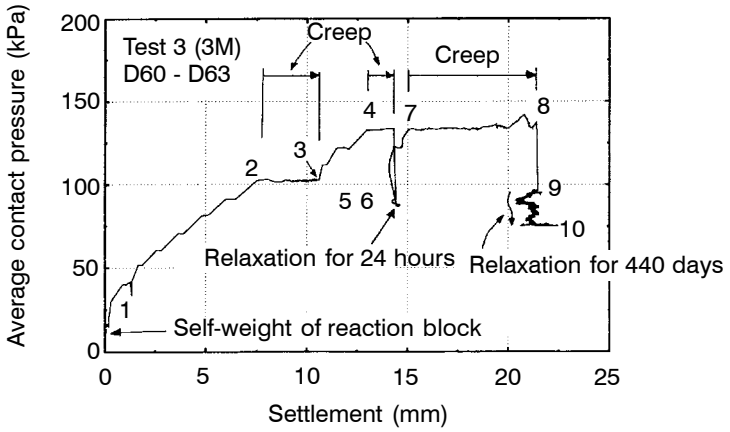

Figure 30. Relationship between the average contact pressure, $(P_0 + P_C)/A$, and the average settlement of the top RC block (test segment 3M).

6. The vertical stiffness of segment 3M during reloading (from Point 6 to Point 7 in Figure 30) is considerably higher than the vertical stiffness at the same load level during primary loading, which is due to the effects of preloading. Furthermore, since segment 3M was reloaded from the prestressed condition (i.e. from Point 6), it is very probable that the stiffness became larger than that during reloading from a lower load level. This is due to the effects of prestressing (this statement is confirmed in Section 5.2.4 using the results from loading tests on a prototype PLPS GRS bridge pier).

The results discussed above are quite encouraging. In particular, it is very important that the relaxation rate of the prestress load significantly reduces due to the creep deformation during the preloading stage. Furthermore, in actual projects, the backfill can be compacted to a denser state. In fact, for field compaction tests using the same type of gravel and a heavy compaction machine, a dry unit weight of 20.5 kN/m^3 was easily achieved (Sekine et al. 1996).

5.2.4 *The First Application of the PLPS Method*

The first application of the PLPS method (Figure 31) was under way at the time of writing at Location 57 in Figure 3 (PLPS GRS-RW site in Figure 15). For this project, a temporary bridge was constructed in 1996 and will be used for several years during the reconstruction of an existing bridge over a small river for a railway on the Sasa-guri Line. Two 16.5 m long steel girders for a single track which have a total weight of 390 kN are supported by a GRS bridge abutment at one end (A2 in Figure 31a), a PLPS GRS bridge pier at the center of the river channel (P1), and an abutment directly supported by cement-treated columns at the other end (A1) (A2 and P1 are instrumented). A soft clay deposit beneath the GRS pier was strengthened by creating in-place columns of cement-treated clay. The authors' main concern is the operational rigidity of the GRS bridge pier against dead and live loads, which are considered in the design to be 196

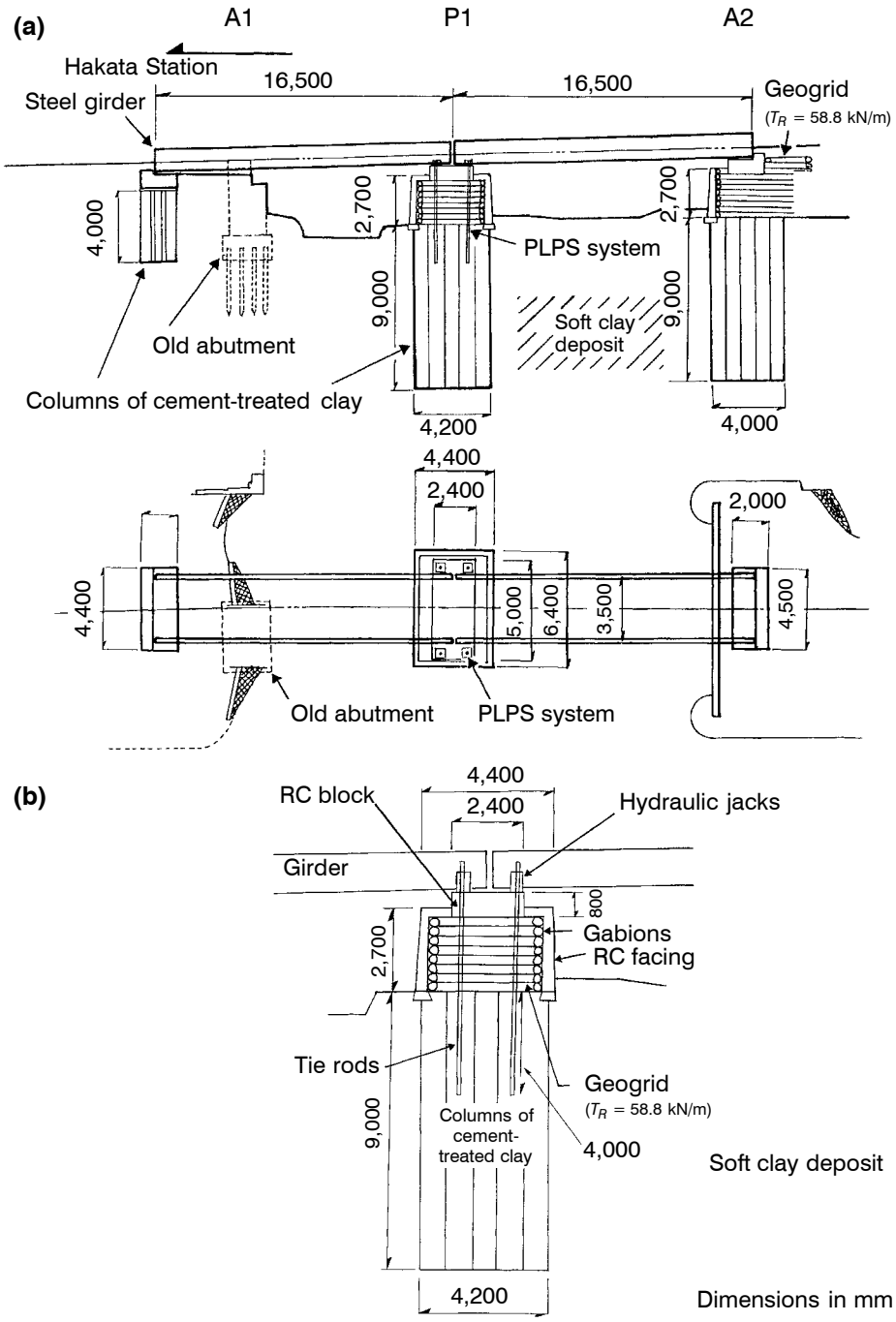

Figure 31. The first PLPS GRS bridge pier located on the Sasa-guri Line (Location 57, Figure 3) (temporary structure): (a) cross section and plan view; (b) detailed schematic of the pier.

kN and 1280 kN, respectively, and the effects of the live load on the relaxation rate of prestress over a long period of time. This temporary structure will provide an excellent opportunity to examine the feasibility of the PLPS method for permanent structures.

The backfill of the PLPS GRS pier is a well-compacted and well-graded gravel of imported crushed sandstone. The reinforcement is a PVA geogrid coated with PVC and has a nominal rupture strength of 73.5 kN/m and a nominal stiffness of 1050 kN/m at strains less than 1%. Alternating vertical reinforcement spacings of 200 and 100 mm, with an average of 150 mm, were used for conservatism (Figure 32a). The bottom ends of the tie rods were anchored into the cement-treated columns. Figures 32c and 32d

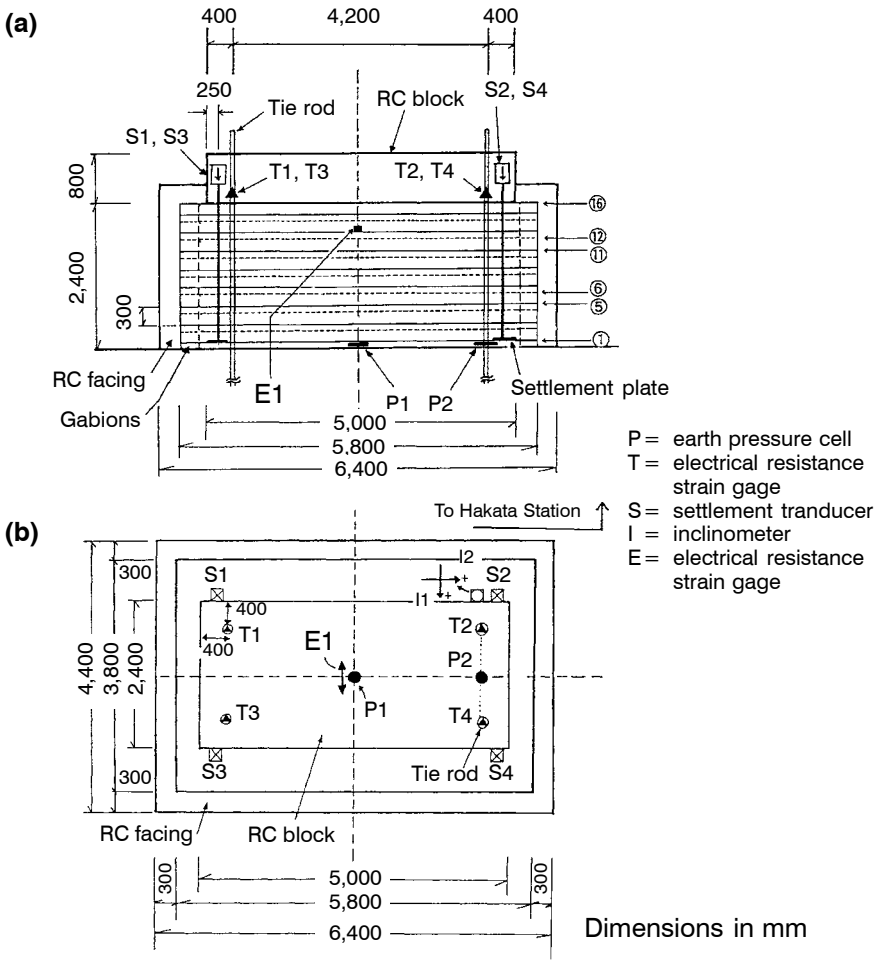

Figure 32. PLPS GRS instrumented bridge pier on the Sasa-guri Line (Location 57, Figure 3), Fukuoka, Kyushu: (a) typical cross section ; (b) plan view (Uchimura et al. 1996, 1997; Tatsuoka and Uchimura 1997b).

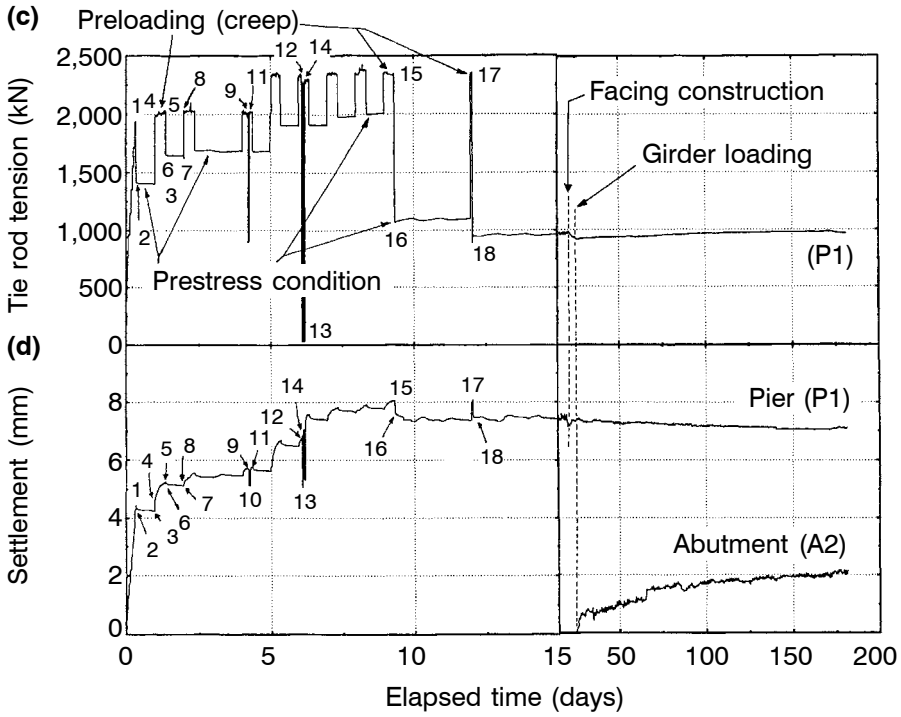

Figure 32 continued. Time histories of: (c) tie rod tension in the pier (P1); (d) settlement of the top reaction block (5 m × 2.4 m in area) of the pier (P1) and the top RC block (4.5 m × 2 m in area) of the GRS bridge abutment (A2) relative to the bottom of the backfill.

show the behavior of the PLPS GRS bridge pier during preloading, and for a period of time after construction. The preload was applied using four hydraulic jacks for only 10 weekdays during daylight hours due to construction restraints at the site (Figure 32c); the total preloading time was 72 hours. The top ends of the four tie rods were fixed to the top reaction block during the night (i.e. during the relaxation stage). Before each relaxation stage started, the tie rod tension dropped by an uncontrolled value (i.e. unloading started). After reaching a load level of 2,400 kN, two complete unloading and reloading cycles were applied. Lastly, the tie rod tension was decreased to approximately 1,000 kN, reloaded and unloaded to the same load level, and then a long-term relaxation stage was started (Stage 18 in Figures 32c and 32d).

The settlement of the top reaction block relative to the bottom of the backfill (i.e. the compression of the backfill) is shown in Figure 32d. Figure 32e shows the relationship between the tie rod tension T, which is equivalent to the vertical load, P_C, applied to the top of the reaction block when $T = 0$, and the settlement of the top reaction block, S. The step-wise relation that exists between T and S during primary loading is due to an incremental increase in the tie rod tension, T; an increment of T of approximately 200 kN was applied for 2 minutes and then the same load level was held for 30 minutes (for

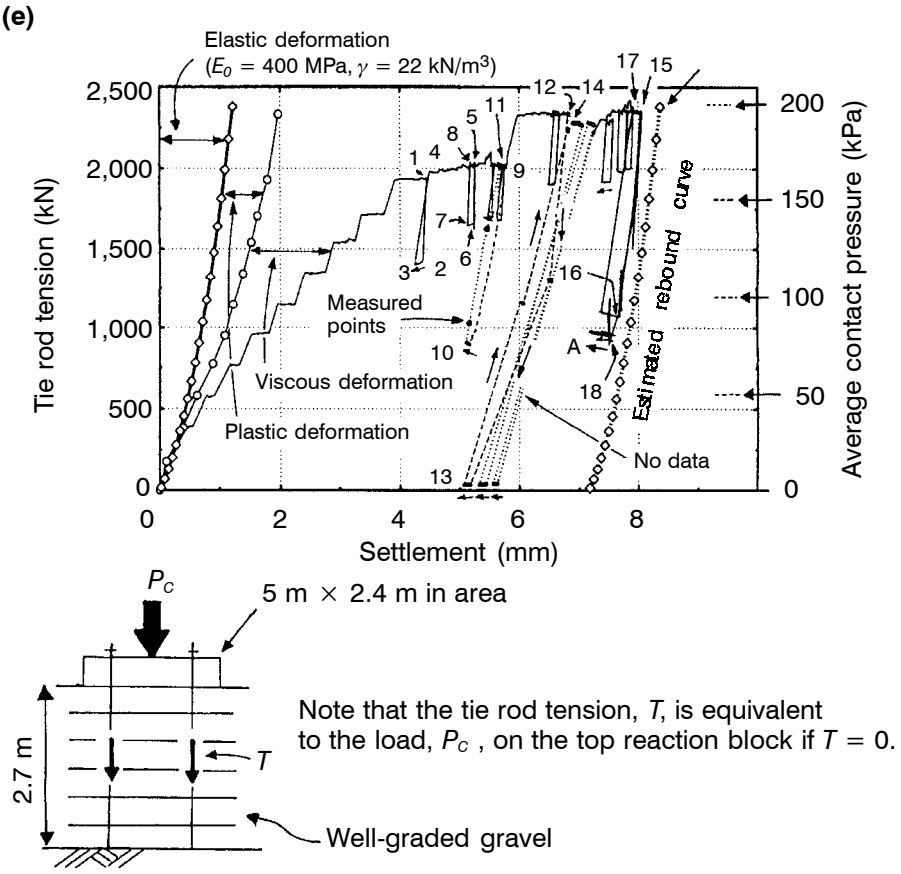

Figure 32 continued. (e) relationship between tie rod tension and settlement of the top reaction block.

the first four steps) or 60 minutes (for all subsequent steps). This procedure was repeated until an approximate load T of 2,000 kN was reached.

Upon inspection of Figure 32e the following trends are identified:

1. The reloading settlement, S, was only 0.4 mm when the load, T (P_C), was increased from 1,000 to 2,400 kN (from Stage 16 to 17). This indicates a significantly high stiffness and is considered to be very satisfactory. When the load T is assumed to be supported by the backfill within the area of the top reaction block, a secant Young's modulus, E_{sec} , of the backfill equal to approximately 400 MPa is obtained. This is a high E_{sec} value that can be achieved only when the backfill is in a near elastic state.
2. A laboratory triaxial test was performed to evaluate the elastic deformation characteristics of the gravel using the method described by Uchimura et al. (1996). Local strains in the triaxial test were measured to an accuracy of 0.0001% because vertical strains in the backfill soil caused by cyclic load applications (which have an ampli-

tude of approximately 1,000 kN, as between Stages 15 and 17, and are similar to the design maximum live load), are only approximately 0.5 mm/2700 mm × 100 = 0.019%. It was found that the elastic Young's modulus, E_v , can be calculated as:

$$E_v = E_0 (\sigma_v/\sigma_0)^m \quad (2)$$

where E_0 (= 400 MPa) is the value of E_v when the vertical stress, σ_v , is equal to the reference pressure, σ_0 (= 98 kPa), and m = 0.5 (refer to Uchimura et al. 1996; Tatsuoka et al. 1997b; Jiang et al. 1997 for more details with regard to Equation 2). The estimated rebound curve obtained based on Equation 2 is presented in Figure 32e. It may be noted that between Stages 15 and 16, the tangent modulus, $K_{tan} = \partial T/\partial S$, decreases as the load T decreases, as suggested by Equation 2. Although only discrete data points are available, the behavior from Stages 12 to 13 is similar.

3. The settlement, S, observed during primary loading consists of elastic reversible deformation and irreversible deformation. The latter consists of plastic (time-independent, irreversible) deformation and viscous (time-dependent) deformation. The viscous deformation presented in Figure 32e was obtained using integration of the settlement increments observed when the load, T, was kept constant. It can be seen that a large part of the initial settlement is viscous. This viscous deformation can be eliminated if a proper preloading procedure is used.
4. The secant stiffness modulus value, $K_{sec} = \Delta T/\Delta S$, is very high and similar to the K_{sec} value during unloading when the pier is reloaded after a small partial unloading (e.g. when reloaded from Stage 3 to 4 after unloading from Stage 1 to 2). As the amount of unloading becomes larger, K_{sec} decreases (i.e. when reloaded from Stage 10 to 11). In particular, the K_{sec} value when reloaded from the zero-load state (e.g. from Stage 13 to 14), is very low. This phenomenon is likely due to the swelling effect of the soil illustrated in Figure 22a. It is interesting to note that at the same load level T, the K_{tan} value during reloading becomes smaller as the amount of unloading increases. This is likely due to the residual tensile force introduced in the reinforcement by preloading and subsequent unloading (Figure 22b). This result clearly demonstrates that a large part of the benefit obtained by preloading is lost by the subsequent unloading to zero load.

Tensile strains in the geogrid were measured at many locations. Figures 32f and 32g show the measured tensile strain at Point E1 (see Figure 32a). It can be seen that for a time period during the first relaxation stage (i.e. from Stage 2 to 3), the tensile geogrid strains typically decreased with time, despite the fact that the load, T, was maintained at an approximately constant value. This trend is opposite to what can be expected if creep was a problem for GRS structures.

For a time period of approximately 160 days after the start of the relaxation stage (i.e. after Stage 18), creep recovery was observed (Figure 33). That is, as denoted by the letter A with an arrow in Figure 32e, with the top of the tie rods fixed to the top reaction block, the tie rod tension, T, increases with time (as seen from Figure 32c) while the backfill is expanding vertically (as seen from Figure 32d) at a slope determined by the stiffness of the tie rods. This result also demonstrates that creep deformation of PLPS GRS structures does not need to be considered in design.

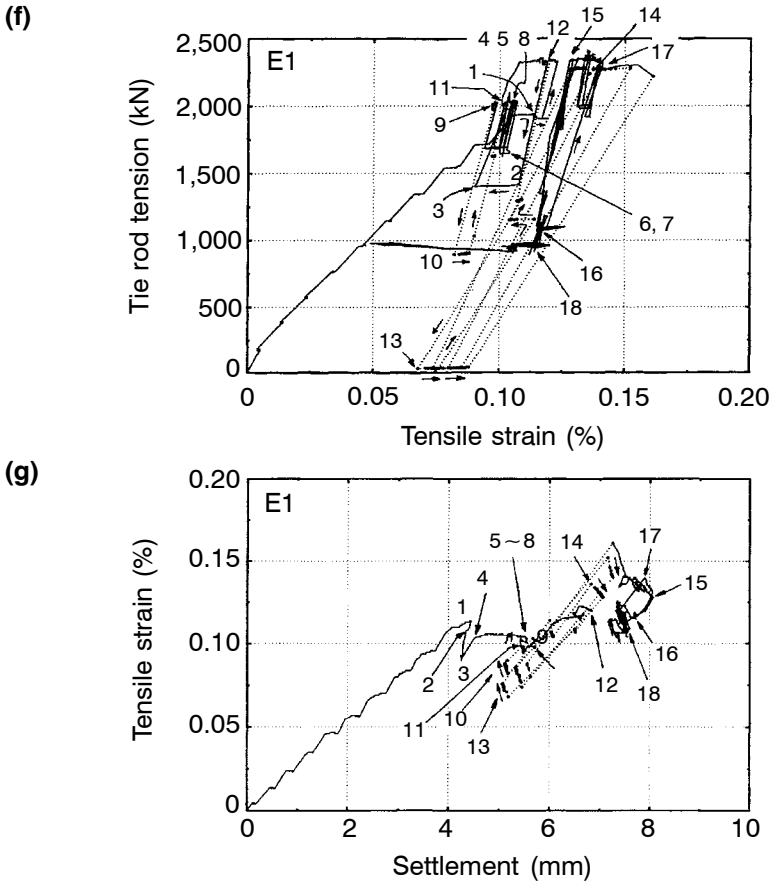

Figure 32 continued. (f) relationship between the tensile strain at E1 (see Figure 32a) and the tie rod tension; (g) relationship between the tensile strain at E1 and the settlement of the top reaction block.

Finally, the settlements of the PLPS GRS pier and the GRS bridge abutment during and after placement of the pair of bridge girders are shown in Figure 32d. The instantaneous settlement of the pier (P1) was 0.08 mm for a girder load of 200 kN while that of the abutment (A2) was 0.5 mm for a girder load of 100 kN. It is very important to note that creep deformation still continues to occur in the abutment (A2). After loading the girders for approximately 160 days, the settlement of the abutment (A2) is 2 mm, while the PLPS pier (P1) has expanded slightly in the vertical direction. These large effects observed in the PLPS GRS bridge pier are quite encouraging.

Despite the above observations, it is likely that the tie rod tension, *T*, may decrease over a long period of time due to the gradual vertical compression of the backfill caused by a continuous application of live cyclic loads (i.e. a train load). A potential construction method that may alleviate this problem would be the use of a connection device between the top end of each rigid tie rod and the top reaction block which would act

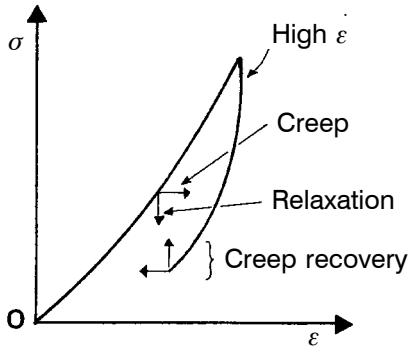

Figure 33. Schematic diagram describing creep recovery.

as a soft spring when the height of the backfill decreases. This method is equivalent to the use of a flexible tie rod with a rigid connection. Using this method, the prestress may decrease only slightly when the backfill is compressed vertically (Tatsuoka et al. 1997b). However, if only this method is used, the advantage of using tie rods, which restrains the movement due to dilation of the densely compacted backfill when sheared laterally, is lost. This problem could be solved by using rigid tie rods with connection devices that perform rigidly when the backfill dilates, and softly when the backfill is compressed (e.g. a ratchet system). This method is currently being studied by the authors.

5.2.5 *Other Possible Applications of the PLPS Method*

The PLPS method can be used to increase the vertical subgrade reaction of level ground to support a heavy structure that can tolerate only limited displacements. In addition, this method is effective not only for compressive loads, but also for tensile loads. Therefore, the rocking motion of a tall structure constructed on PLPS reinforced soil could be effectively restrained (Tatsuoka et al. 1997b).

6 SEISMIC STABILITY OF REINFORCED SOIL RETAINING WALLS

6.1 General

At 5:46 a.m. on 17 January 1995, a devastating earthquake measuring 7.2 on the Richter scale occurred in the southern section of Hyogo Prefecture, including Kobe City and neighboring urban areas. In the severely affected areas (Figure 34), an extensive length of railway embankments had been constructed more than seventy years before the earthquake, which had a number of old and new retaining walls. Most of the walls were seriously damaged. The details have been reported by Tatsuoka et al. (1996a, 1996b). The conventional types of retaining walls can be categorized into four groups:

1. masonry retaining walls (denoted by MS in Figure 34);

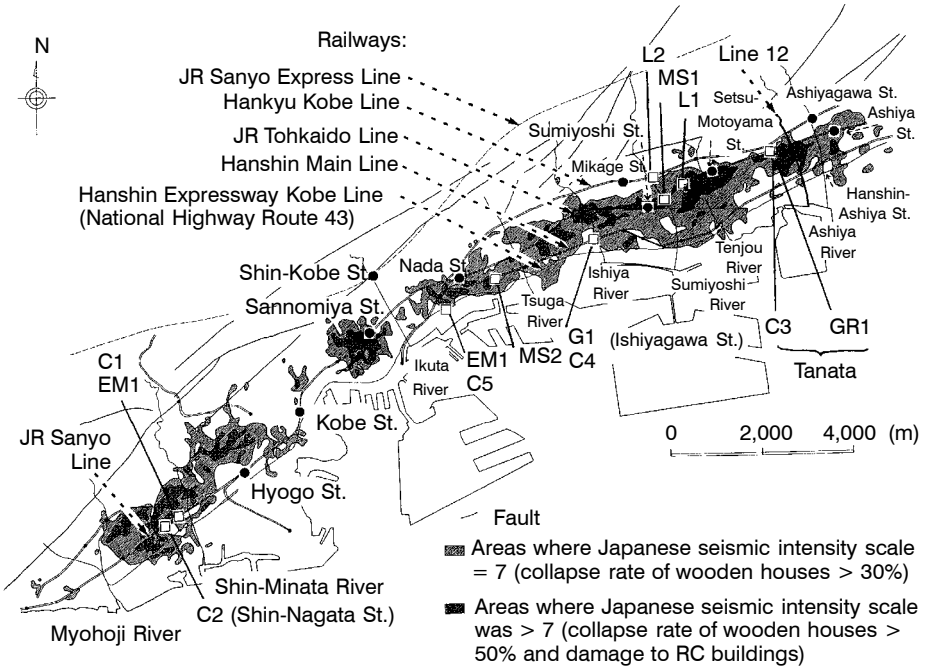

Figure 34. Seriously damaged areas during the 1995 Great Hanshin Earthquake (modified from Chuo Kaihatsu Corporation 1995).
Note: EM = damaged embankments.

2. leaning (supported), unreinforced concrete retaining walls (L);
3. gravity, unreinforced concrete retaining walls (G); and
4. cantilever or inverted T-shaped steel-reinforced concrete (RC) retaining walls (C).

The first three types of retaining walls were the most seriously damaged, while the damage to cantilever walls was generally less serious.

6.2 Tanata Wall

Despite the fact that the seismic intensity at this site was severe, the damage to a GRS-RW with a FHR facing located at Tanata (GR1 in Figure 34) was significantly less serious when compared to the damage experienced by the four types of retaining walls described in Section 6.1 (Figure 35). The Tanata wall was completed in February 1992 on the southern slope of an existing embankment for the JR Kobe Line to increase the number of railway tracks from four to five. The total wall length is 305 m and the greatest height is 6.2 m. The surface layer in the subsoil consists of relatively stiff terrace soils (Figure 35b). The backfill soil is basically a cohesionless soil with a small amount of fines. The reinforcement is a geogrid (PVA) coated with soft PVC for protection, and

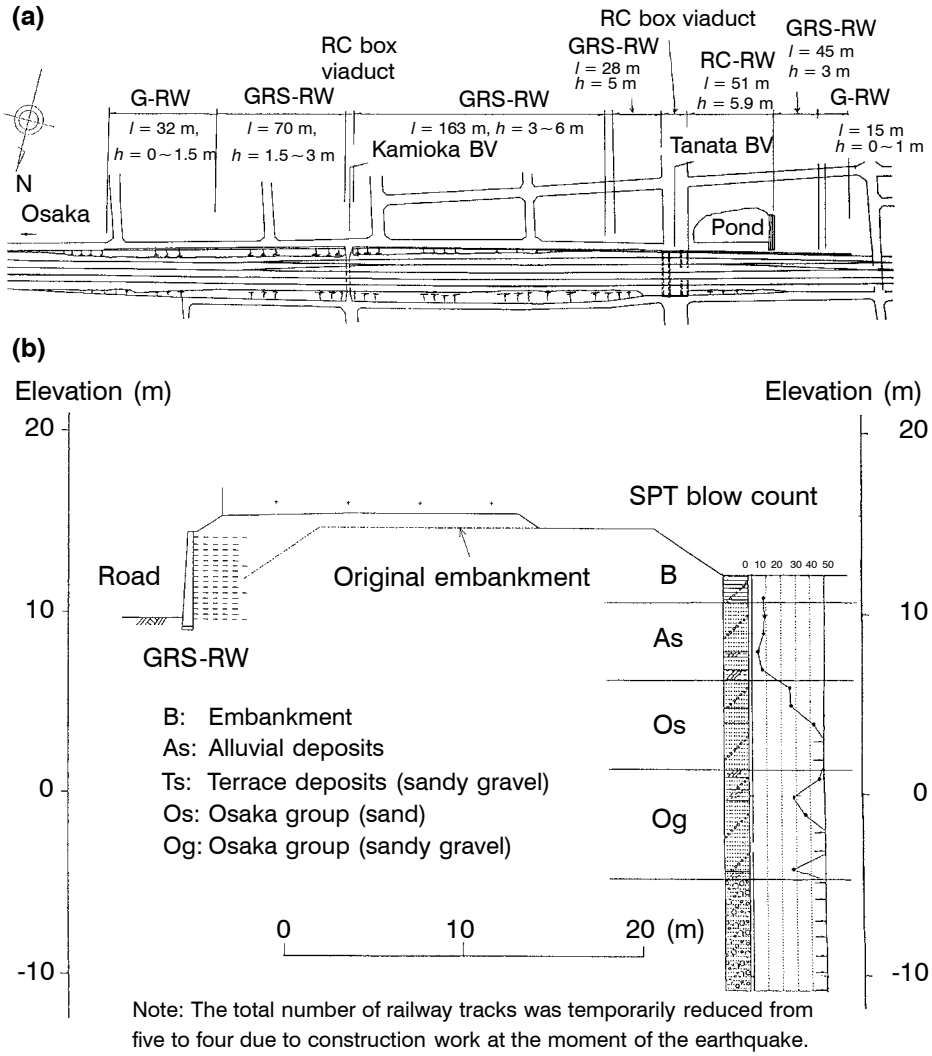

Figure 35. Tanata wall: (a) plan view (G-RW = gravity retaining wall); (b) cross section of the embankment.

has a nearly rectangular cross section of 2 mm by 1 mm and an aperture size of 20 mm with a nominal tensile rupture strength, T_R = 30.4 kN/m.

This wall deformed and moved slightly laterally in an outward direction. The largest outward displacement occurred at the highest wall location, which is in contact with a RC box culvert structure crossing the railway embankment. The displacement was 260 mm and 100 mm at the top of the wall and at ground level, respectively (Figure 36a).

(c)

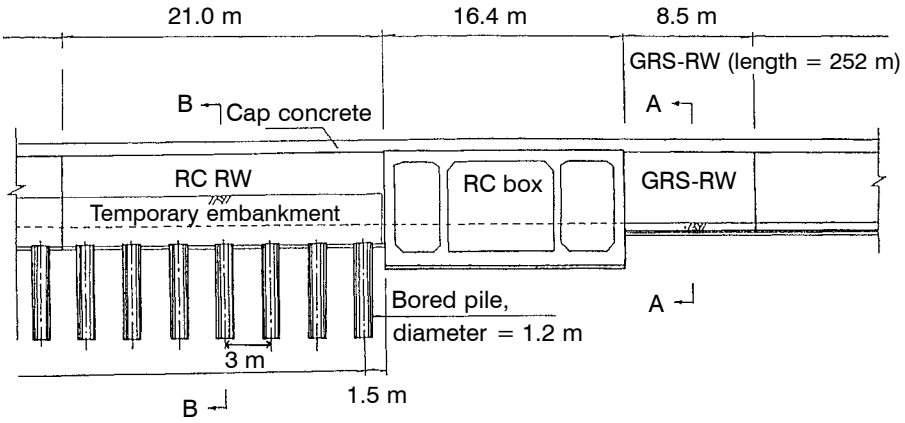

(d)

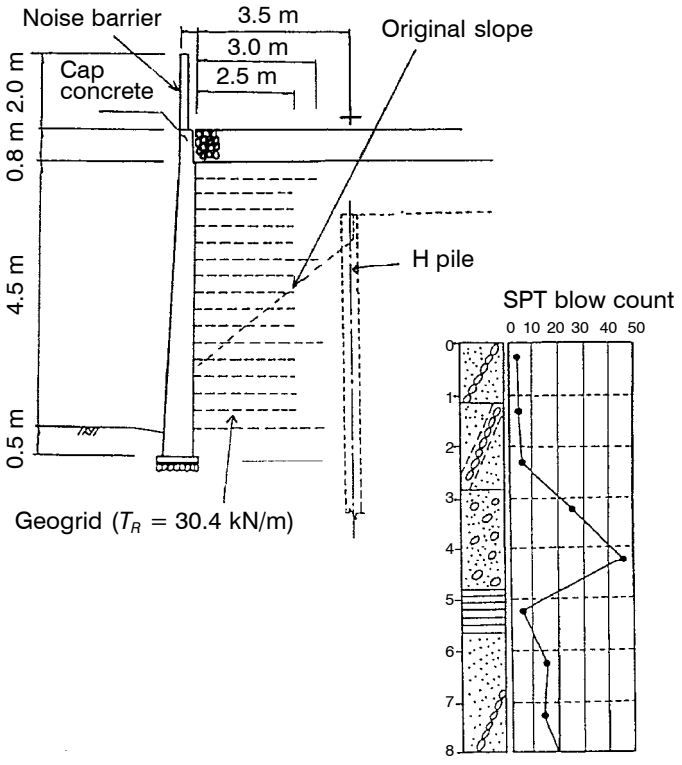

Figure 35 continued. (c) front view (from the south) of the GRS-RWs and RC retaining walls supported by a pile foundation; (d) typical cross section of a GRS-RW.

(a)

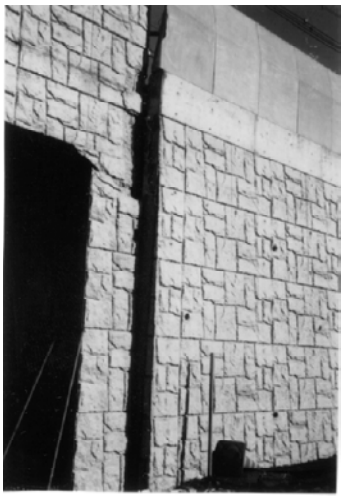

(b)

Figure 36. Tanata wall immediately after the earthquake: (a) front view; (b) side view showing collapsed wooden houses.

Based on the following facts and despite the above observations, the performance of the GRS-RW was considered satisfactory by the railway engineers responsible for this structure:

- The peak ground acceleration at the site was estimated to be more than 700 gals (0.7g). This is confirmed by the high collapse rate of wooden houses at the site (Figure 36b). Many of the collapsed houses were constructed less than approximately ten years ago.
- On the opposite side of the RC box structure, a RC retaining wall with a maximum height of approximately 5.4 m (Figure 37) had been constructed concurrently with the GRS-RW. This wall is supported by a row of bored piles despite the similar subsoil conditions as the GRS-RW. Therefore, the construction cost per wall length of the RC

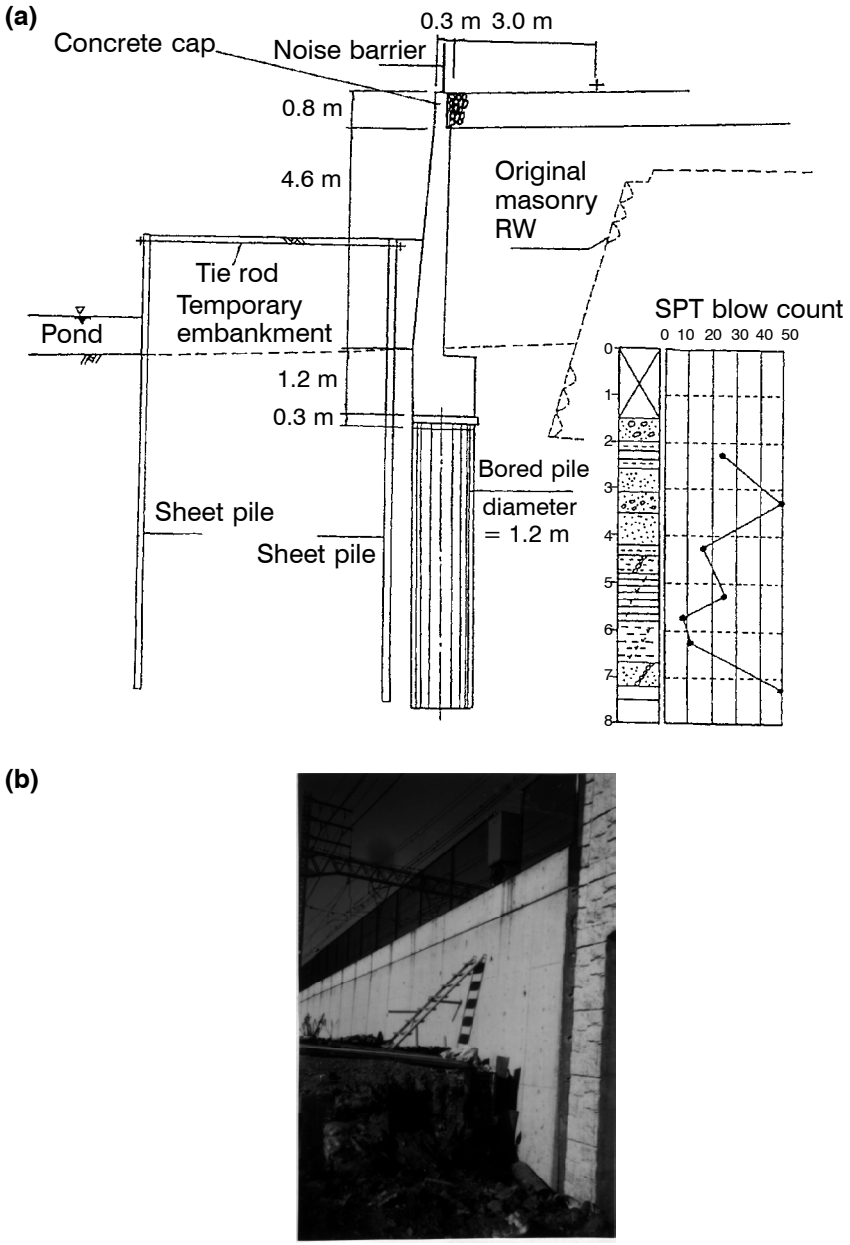

Figure 37. RC retaining wall at Tanata: (a) cross section; (b) front view.

retaining wall was approximately double to triple of that for the GRS-RW. In addition, a temporary cofferdam still existed at the time of the earthquake in front of the RC

retaining wall. This may have contributed to the stability of the RC retaining wall during the earthquake. Despite these differences, the RC retaining wall displaced similarly to the GRS-RW (Figure 37b), i.e. at the interface with the RC box structure, the outward lateral displacement of the retaining wall was 215 mm at the top and 100 mm at ground level.

- The length of geogrid reinforcement used in GRS-RWs with FHR facings is generally shorter than that for most metal strip-reinforced soil retaining walls and other types of GRS retaining walls with deformable facings. For conservatism, most of the GRS-RWs with FHR facings constructed to date have several longer reinforcement layers at high wall levels (Figures 2a and 38). For the Tanata wall, the length of all reinforcement layers were truncated to approximately the same length due to construction restraints at the site (Figure 35d). This arrangement may have reduced the seismic stability of the wall; the wall would have tilted less if the top geogrid layers had been made longer.

6.3 Other GRS-RWs With FHR Facings

In addition to the Tanata GRS-RW, the following GRS-RWs with FHR facings were constructed at three other locations where the seismic intensity was five or six on the Japanese intensity scale and a number of wooden houses, railway and highway embankments, and conventional retaining walls were seriously damaged; however, these GRS-RWs were not damaged (Tatsuoka et al. 1996b):

- The Amagasaki No. 1 wall (Kanazawa et al. 1994) is the first large-scale construction project of the GRS-RW system to directly support the tracks of a very busy railway (Kobe Line, Figure 38). The average wall height is 5 m and the total length is 1,300

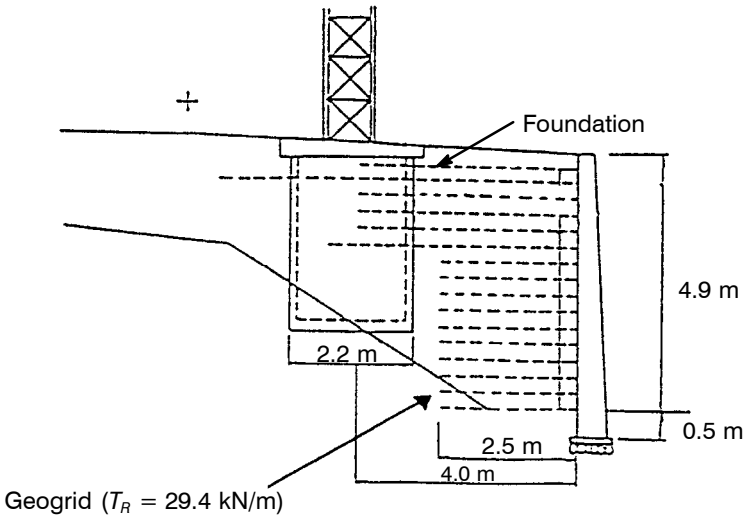

Figure 38. Typical cross section of GRS-RWs for the Kobe Line in Amagasaki (Location 7, Figure 3).

m. At a few locations along the wall, foundations for steel frame structures for an electric power supply were constructed inside the reinforced zone. Four pairs of GRS bridge abutments were also constructed to directly support bridge girders.

- Walls having a maximum height of 6.3 m and a total length of 120 m at the Maiko site in Tarumi-ku, Kobe City, were completed in May 1993 in order to expand the top of the road adjacent to one of the approach roads to the Akashi Kaikyo (Strait) Bridge, which was under construction at the time of the earthquake. This site is located only 5 km from the earthquake epicenter.
- The Amagasaki No. 2 wall with a height of 3 to 8 m and a length of approximately 400 m, located west of the Amagasaki No. 1 GRS-RW. The wall was completed in March 1994 to support a new approach fill for a JR bridge on the Fukuchiyama Line.

One of the mechanisms that makes GRS-RWs with FHR facings much more stable against seismic forces than conventional gravity retaining walls is that the reinforced zone can behave as a relatively flexible monolithic mass with a relatively large width/height ratio. For additional discussions with regard to the seismic stability of GRS-RW systems, refer to Tatsuoka et al. (1996b).

7 SUMMARY

The GRS-RW system discussed in this paper has been used to construct important permanent retaining walls and bridge abutments in Japan to a much greater extent and at a much higher rate than anticipated when the study of GRS-RW systems began in 1982. Thus far, these GRS-RW systems have mainly been constructed as railway support structures. The authors believe that their use is due not only to their cost-effectiveness, but also that their performance is equivalent to, or better than that of, other modern reinforced concrete retaining walls and reinforced concrete bridge abutments. One of the prime reasons for the success of GRS-RW systems is the use of the proper type of geosynthetic (a geogrid for cohesionless soils or a nonwoven/woven geotextile composite for nearly saturated cohesive soils), and the use of full-height rigid (FHR) facings that are cast in place using staged construction procedures.

It is anticipated that the new construction method of preloading and prestressing will assist in exploring new applications of GRS-RWs for bridge abutments and piers that can tolerate only very small displacements.

ACKNOWLEDGMENT

The authors deeply appreciate the cooperation provided by their previous and current colleagues at the University of Tokyo and the Railway Technical Research Institute in performing this long-term investigation.

REFERENCES

Chuo Kaihatsu Corporation, 1995, "*Report of Damage Investigation for the Great Hanshin Earthquake, No. 2 - Damage Ratio Investigation and Geology and Ground Conditions*", Japan. (in Japanese)

Doi, Y., Mizushima, S., Tateyama, M. and Murata, O., 1994, "Geotextile-Reinforced Soil Retaining Wall; Reconstruction of a Railway Embankment at Rokujizo, Kyoto", *Recent Case Histories of Permanent Geosynthetic-Reinforced Soil Retaining Walls*, Tatsuoka, F. and Leshchinsky, D., Editors, Balkema, 1994, Proceedings of Seiken Symposium No. 11, Tokyo, Japan, November 1992, pp. 197-204.

Horii, K., Kishida, H., Tateyama, M. and Tatsuoka, F., 1994, "Computerized Design Method for Geosynthetic-Reinforced Soil Retaining Walls for Railway Embankments", *Recent Case Histories of Permanent Geosynthetic-Reinforced Soil Retaining Walls*, Tatsuoka, F. and Leshchinsky, D., Editors, Balkema, 1994, Proceedings of Seiken Symposium No. 11, Tokyo, Japan, November 1992, pp. 205-218.

Huang, C-C. and Tatsuoka, F., 1990, "Bearing Capacity of Reinforced Level Ground", *Geotextiles and Geomembranes*, Vol. 9, No. 1, pp. 51-82.

Huang, C-C., Tatsuoka, F. and Sato, Y., 1994, "Failure Mechanisms of Reinforced Sand Slopes Loaded With a Footing, *Soils and Foundations*, Vol. 34, No. 2, pp. 27-40.

Jewell, R.A., 1990, "Strength and Deformation in Reinforced Soil Design", *Proceedings of the Fourth International Conference on Geotextiles, Geomembranes and Related Materials*, Keynote Lecture, Balkema, Vol. 3, The Hague, The Netherlands, May 1990, pp. 913-946.

Jiang, G.L., Tatsuoka, F., Flora, A. and Koseki, J., 1997, "Inherent and Stress State-Induced Anisotropy in Small Strain Stiffness of a Sandy Gravel", *Géotechnique*, Special Issue, Symposium, to be published.

Kanazawa, Y., Ikeda, K., Murata, O., Tateyama, M. and Tatsuoka, F., 1994, "Geosynthetic-Reinforced Soil Retaining Walls for Reconstructing Railway Embankment at Amagasaki", *Recent Case Histories of Permanent Geosynthetic-Reinforced Soil Retaining Walls*, Tatsuoka, F. and Leshchinsky, D., Editors, Balkema, 1994, Proceedings of Seiken Symposium No. 11, Tokyo, Japan, November 1992, pp. 233-242.

Ling, H.I. and Tatsuoka, F., 1994, "Performance of Anisotropic Geosynthetic-Reinforced Cohesive Soil Mass", *Journal of Geotechnical Engineering*, ASCE, Vol. 120, No. 7, pp. 1166-1184.

Ling, H.I., Tatsuoka, F. and Tateyama, M., 1995, "Simulating the Performance of GRS-RW by Finite Element Procedure", *Journal of Geotechnical Engineering*, ASCE, Vol. 124, No. 4, pp. 330-340.

Mitchell, J.K. and Zornberg, J.G., 1995, "Reinforced Soil Structures With Poorly Draining Backfills: Part II", *Geosynthetics International*, Vol. 2, No. 1, pp. 265-307.

Murata, O., Tateyama, M. and Tatsuoka, F., 1994, "Shaking Table Tests on a Large Geosynthetic-Reinforced Soil Retaining Wall Model", *Recent Case Histories of Permanent Geosynthetic-Reinforced Soil Retaining Walls*, Tatsuoka, F. and Leshchinsky, D., Editors, Balkema, 1994, Proceedings of Seiken Symposium No. 11, Tokyo, Japan, November 1992, pp. 259-264.

Murata, O., Tateyama, M., Tatsuoka, F., Nakamura, K. and Tamura, Y., 1991, "A Reinforcing Method for Each Retaining Walls Using Short Reinforcing Members and a Continuous Rigid Facing", *Geotechnical Engineering Congress 1991*, McLean, F., Campbell, D.A. and Harris, D.W., Editors, ASCE Geotechnical Special Publication No. 27, Vol. 2, Proceedings of a congress held in Boulder, Colorado, USA, June 1991, pp. 935-946.

Schlosser, F., Delmas, P. and Unterreiner, P., 1994, "Utilization of Geosynthetics and Natural Fibers in Geotechnical Engineering", *Proceedings of the Thirteenth International Conference on Soil Mechanics and Foundation Engineering*, Vol. 6, New Delhi, India, January 1994, pp. 89-96.

Sekine, E., Murata, O., Kohata, Y., Yazaki, S., Abe, N. and Maruyama, T., 1996, "Rolling Compaction Test for Railway Embankment on Gravel", *Proceedings of the Thirty-First Japan National Conference on Geotechnical Engineering*, Japanese Geotechnical Society, Vol. 2, pp. 2339-2340.

Tada, N., Tamura, Y., Sasaki, T., Misono, K. and Hosoi, T., 1997, "Widening the Road from Existing Two Lanes to Four Lanes by Geotextile-Reinforced Retaining Wall at Yamagata Super Highway", *Proceedings of the Thirty-Second Japan National Conference in Geotechnical Engineering*, Kumamoto, Japan, to be published. (in Japanese)

Tajiri, N., Tsukada, Y., Yamamoto, M., Ochiai, Y. and Dobashi, K., 1996, "Comparison Among Full-Scale Failure Experiments of Geotextile Reinforced Soil Walls with Different Facing Types", *Proceedings of the Tenth Japanese Geotextile Symposium*, IGS Japanese Chapter, to be published. (in Japanese)

Tamura, Y., Nakamura, K., Tatsuoka, F., Tateyama, M., Murata, O. and Nakaya, T., 1994, "Full-Scale Lateral Loading Tests on Column Foundations in Geosynthetic-Reinforced Soil Retaining Walls", *Recent Case Histories of Permanent Geosynthetic-Reinforced Soil Retaining Walls*, Tatsuoka, F. and Leshchinsky, D., Editors, Balkema, 1994, Proceedings of Seiken Symposium No. 11, Tokyo, Japan, November 1992, pp. 277-285.

Tateyama, M., Murata, O., Tatsuoka, F., Tamura, Y., Nakamura, K. and Nakaya, T., 1994a, "Lateral Loading Tests on Columns on the Facing of Geosynthetic-Reinforced Soil Retaining Walls", *Recent Case Histories of Permanent Geosynthetic-Reinforced Soil Retaining Walls*, Tatsuoka, F. and Leshchinsky, D., Editors, Balkema, 1994, Proceedings of Seiken Symposium No. 11, Tokyo, Japan, November 1992, pp. 287-294.

Tateyama, M., Murata, O., Watanabe, K. and Tatsuoka, F., 1994b, "Geosynthetic-Reinforced Retaining Walls for Bullet Train Yard in Nagoya", *Recent Case Histories of Permanent Geosynthetic-Reinforced Soil Retaining Walls*, Tatsuoka, F. and Leshchinsky, D., Editors, Balkema, 1994, Proceedings of Seiken Symposium No. 11, Tokyo, Japan, November 1992, pp. 141-150.

Tatsuoka, F., 1993, "Roles of Facing Rigidity in Soil Reinforcing", *Earth Reinforcement Practice*, Keynote Lecture, Ochiai, H., Hayashi, S. and Otani, J., Editors, Balkema, 1993, Proceedings of the International Symposium on Earth Reinforcement Practice, IS Kyushu '92, Vol. 2, Kyushu, Fukuoka, Japan, November 1992, pp. 831-870.

Tatsuoka, F., Ando, H., Iwasaki, K. and Nakamura, K., 1986, "Performance of Clay Test Embankments Reinforced With a Non-Woven Geotextile", *Proceedings of the Third International Conference on Geotextiles*, Vol. 3, Vienna, Austria, April 1986, pp. 355-360.

Tatsuoka, F., Koseki, J. and Tateyama, M., 1996a, "Performance of Reinforced Structures During the 1995 Hyogo-ken Nanbu Earthquake", Special Report, *Earth Reinforcement*, Ochiai, H., Yasufuku, N. and Omine, K., Editors, Proceedings of the International Symposium on Earth Reinforcement, IS Kyushu '96, Vol. 2, Kyushu, Fukuoka, Japan, November 1996, preprint, pp. 105-140.

Tatsuoka, F. and Leshchinsky, D., Editors, 1994, "*Recent Case Histories of Permanent Geosynthetic-Reinforced Soil Retaining Walls*", Balkema, 1994, Proceedings of Seiken Symposium No. 11, Tokyo, Japan, November 1992, 349 p.

Tatsuoka, F., Murata, O. and Tateyama, M., 1992, "Permanent Geosynthetic-Reinforced Soil Retaining Walls Used for Railway Embankment in Japan", *Geosynthetic-Reinforced Soil Retaining Walls*, Wu, J.T.H., Editor, Balkema, 1992, Proceedings of the International Symposium on Geosynthetic-Reinforced Soil Retaining Walls, Denver, Colorado, USA, August 1991, pp. 101-130.

Tatsuoka, F., Murata, O., Tateyama, M., Nakamura, K., Tamura, Y., Ling, H.I., Iwasaki, K. and Yamauchi, H., 1991, "Reinforcing Steep Clay Slopes With a Non-Woven Geotextile", *Performance of Reinforced Soil Structures*, McGown, A., Yeo, K. and Andrawes, K.Z., Editors, Thomas Telford, 1991, Proceedings of the International Reinforced Soil Conference held in Glasgow, Scotland, September 1990, pp. 141-146.

Tatsuoka, F., Pradhan, T.B.S. and Yoshi-ie, H., 1989a, "A Cyclic Undrained Simple Shear Testing Method for Soils", *Geotechnical Testing Journal*, ASTM, Vol. 12, No. 4, pp. 269-280.

Tatsuoka, F., Tamura, Y., Nakamura, K., Iwasaki, K. and Yamauchi, H., 1987, "Behavior of Steep Slope Clay Embankments Reinforced With a Non-Woven Geotextile Having Various Face Structures", *Proceedings of the Post Vienna Conference on Geotextiles*, Singapore, pp. 387-403.

Tatsuoka, F., Tateyama, M. and Koseki, J., 1996b, "Performance of Soil Retaining Walls for Railway Embankments", *Soils and Foundations*, Special Issue for the 1995 Hyogoken-Nambu Earthquake, pp. 311-324.

Tatsuoka, F., Tateyama, M. and Murata,O., 1989b, "Earth Retaining Wall With a Short Geotextile and a Rigid Facing", *Proceedings of the Twelfth International Conference on Soil Mechanics and Foundation Engineering*, Balkema, 1992, Vol. 2, Rio de Janeiro, Brazil, August 1989, pp. 1311-1314.

Tatsuoka, F., Tateyama, M., Murata, O. and Tamura, Y., 1994, "Closure to the Discussion by Mr. Pierre Segrestin on 'Geosynthetic-Reinforced Soil Retaining Walls With Short Reinforcement and a Rigid Facing'", *Recent Case Histories of Permanent Geosynthetic-Reinforced Soil Retaining Walls*, Tatsuoka, F. and Leshchinsky, D., Editors, Balkema, 1994, Proceedings of Seiken Symposium No. 11, Tokyo, Japan, November 1992, pp. 323-344.

Tatsuoka, F., Tateyama, M., Tamura, Y. and Yamauchi, H., 1997a, "Lessons Learned from the Failures of a Series of Full-Scale Geosynthetic-Reinforced Soil Retaining Walls", *Geosynthetics: Lessons Learned from Failures*, IFAI, Giroud et al., Editors, to be published.

Tatsuoka, F. and Uchimura, T., 1997a, "Discussion 'Why is PS Required in Addition to PL?'", *Proceedings of the International Symposium on Mechanically Stabilized Backfill*, Balkema, Denver, Colorado, USA, February 1997, to be published.

Tatsuoka, F. and Uchimura, T., 1997b, "Discussion Points for Panel Discussion on Long-Term Deformation of MSB Retaining Walls", *Proceedings of the International Symposium on Mechanically Stabilized Backfill*, Balkema, Denver, Colorado, USA, February 1997, to be published.

Tatsuoka, F., Uchimura, T. and Tateyama, M., 1997b, "Preloaded and Prestressed Reinforced Soil", *Soils and Foundations*, Vol. 3, No. 2, to be published.

Tatsuoka, F., Uchimura, T., Tateyama, M. and Muramoto, K., 1996c, "Creep Deformation and Stress Relaxation in Preloaded/Prestressed Geosynthetic-Reinforced Soil Retaining Walls", *Proceedings of the Session "Measuring and Modeling Time-Dependent Soil Behavior"*, ASCE Geotechnical Special Publication No. 6, Sheahan and Kaliakin, Editors, ASCE Washington Convention, pp. 258-272.

Tatsuoka, F. and Yamauchi, H., 1987, "A Reinforcing Method for Steep Clay Slopes Using a Non-Woven Geotextile", *Geotextiles and Geomembranes*, Vol. 4, pp. 241-268.

Uchimura, T. Tatsuoka, F., Maruyama, D., Nakamura, H., Tateyama, M. and Koga, T., 1997, "Construction of a Prototype Preloaded and Prestressed Reinforced Soil Bridge Pier", *Proceedings of Thirty-Second Japan National Conference on Geotechnical Engineering*, Kumamoto, Japan, to be published. (in Japanese)

Uchimura, T., Tatsuoka, F., Sato, T., Tateyama, M. and Tamura, Y., 1996, "Performance of Preloaded and Prestressed Geosynthetic-Reinforced Soil", *Earth Reinforcement*, Ochiai, H., Yasufuku, N. and Omine, K., Editors, Proceedings of the International Symposium on Earth Reinforcement, IS Kyushu '96, Vol. 1, Kyushu, Fukuoka, Japan, November 1996, pp. 537-542.

Yamauchi, H. and Tatsuoka, F., Nakamura, K., Tamura, Y. and Iwasaki, K., 1987, "Stability of Steep Slope Clay Embankments Reinforced With a Non-Woven Geotextile", *Proceedings of the Post Vienna Conference on Geotextiles*, Singapore, pp. 370-386.

Zornberg, J.G. and Mitchell, J.K., 1994, "Reinforced Soil Structures With Poorly Draining Backfills: Part I", *Geosynthetics International*, Vol. 1, No. 2, pp. 103-148.

NOTATIONS

Basic SI units are given in parentheses.

C = compressive load applied to top of backfill (N/m)

c = soil cohesion (N/m^2)

e = void ratio (Figure 26) (dimensionless)

E_{sec} = secant Young's modulus (Pa)

E_v = Young's modulus calculated as $(\partial \sigma_v / \partial \varepsilon_v^e)$ (Pa)

E_0 = elastic Young's modulus when vertical stress equals atmospheric pressure (i.e. when $\sigma_v = \sigma_0$) (Pa)

G = shear modulus (Pa)

H = noise barrier fence force (Figure 12b) (N)

h = height (Figure 35a) (m)

J = geosynthetic stiffness (N/m)

K_{sec} = secant modulus (Pa)

K_{tan} = tangent modulus (Pa)

k_h = horizontal pseudo-static seismic coefficient (dimensionless)

L_a = anchorage length (Figure 5a) (m)

L_r = retaining length (Figure 5a) (m)

l = length (Figure 35a) (m)

M = overturning moment (Figure 4) (N-m/m)

m = constant (Equation 2) (dimensionless)

P = total vertical load at top of soil mass (N/m)

P_A = active earth pressure (N/m)

P_C = external compressive/vertical load (N/m)

P_W = lateral earth force acting against wall facing (Figure 5a) (N/m)

P_0 = vertical load due to self-weight of RC block (Figure 28) (N/m)

S = settlement (m)

T = tensile force in reinforcement (N/m)

T_c = uniform tensile force along a prestressed anchoring system (Figure 5) (N/m)

T_R = tensile rupture strength of reinforcement (N/m)

T_{anchor} = maximum available anchor capacity of reinforcement (N/m)

T_{max} = maximum available tensile force in reinforcement (N/m)

$T_{(max)A1}$ = maximum tensile force in distribution A1 (Figure 5) (N/m)

$T_{(max)A2}$ = maximum tensile force in distribution A2 (Figure 5) (N/m)

$T_{(max)B1}$ = maximum tensile force in distribution B1 (Figure 5) (N/m)

$T_{(max)B2}$ = maximum tensile force in distribution B2 (Figure 5) (N/m)

T_{retain} = maximum available retaining force (Figure 5) (N/m)

T_W = tensile force in reinforcement at connection between reinforcement and back of facing (Figure 5) (N/m)

T_{Wmax} = maximum tensile force in reinforcement at connection between reinforcement and back of facing (Figure 5) (N/m)

V = sliding force (Figure 4) (N/m)

γ = unit weight of soil (Figure 32e) (N/m^3)
γ_d = dry unit weight of soil (N/m^3)
ε = strain (Figure 33) (dimensionless)
ε_{vol} = volumetric strain (dimensionless)
ε_v^e = major principle elastic (vertical) strain (dimensionless)
$\varepsilon\gamma$ = shear strain (dimensionless)
ε_1 = major principle axial strain (dimensionless)
$\dot{\varepsilon}$ = strain rate (Figure 33) (dimensionless)
σ = normal stress (Figure 33) (Pa)
$(\sigma_h)_{local}$ = local lateral stress (Pa)
σ_v = vertical normal stress (Pa)
σ_{vb} = pressure due to self-weight of concrete blocks (Pa)
$(\sigma_v)_{local}$ = local vertical stress (Pa)
σ_{v0} = pressure due to self-weight of the backfill (Pa)
σ_v' = vertical effective stress (Figure 26) (Pa)
σ_0 = reference pressure (Pa)
σ_1 = major principal stress (Pa)
σ_1' = major principal effective stress (Pa)
σ_2', σ_3' = minor principal effective stresses (Pa)
τ = shear stress (Pa)
ϕ = internal friction angle of soil (°)

ABBREVIATIONS

CJ: construction joint
FHR: full height rigid
GRS-RW: geosynthetic-reinforced soil retaining wall
G-RW: gravity retaining wall
IIS: Institute of Industrial Science
JR: Japan Railways
PL: preloaded
PLPS: preloaded and prestressed
PS: prestressed
PSC: plane strain compression
PVA: polyvinyl alcohol
PVC: polyvinyl chloride
RC: reinforced concrete

RW: retaining wall
SPT: standard penetration test